



ACCELERATOR PRODUCTION OF ^{99m}Tc WITH PROTON BEAMS AND ENRICHED ^{100}Mo TARGETS

M.C. LAGUNAS-SOLAR
University of California,
Davis, California,
United States of America

Abstract

The direct production of ^{99m}Tc has been developed based upon the use of the $^{100}\text{Mo}(p,2n)^{99m}\text{Tc}$ reaction ($Q = -7.9$ MeV), using enriched ^{100}Mo targets and accelerated protons of <25 MeV. Cumulative ^{99m}Tc yields measured in this work reached 851 ± 77 MBq/ $\mu\text{A}/\text{h}$ (23.0 ± 3.0 mCi/ $\mu\text{A}/\text{h}$) at end-of-bombardment (EOB) in the 22-12 MeV energy region, with ^{96}Tc (4.35 d) as the only detectable impurity at <0.0003 % at EOB. By using high-intensity beams (i.e. 1 mA) available from modern H^+ accelerators, and by extracting multiple H^+ beams to bombard a single or an array of enriched ^{100}Mo targets, this method could provide nearly 851 GBq (23 Ci) of ^{99m}Tc in 1-h bombardments. Because of this large-batch potential, this new method appears to be an effective alternative to the production and distribution of $^{99}\text{Mo} \rightarrow ^{99m}\text{Tc}$ generator systems, although it may be limited to daily, regional/local distribution and use. ^{99m}Tc produced in this fashion has high radionuclidic and radiochemical purity, although its specific activity has not been determined. The accelerator-made ^{99m}Tc has been shown to have similar physical and chemical characteristics than ^{99m}Tc eluted from commercial fission-produced $^{99}\text{Mo} \rightarrow ^{99m}\text{Tc}$ generators. Technical and logistical factors need further study and analysis but the potential and the expected impact of this new method are clear in the context of the operation of large radionuclide distribution centers as well as for small programs in developing regions.

1. INTRODUCTION

The use of ^{99m}Tc (6.02 h) in nuclear medicine is well established worldwide. Its supply and distribution is largely based on the use of reactor technologies to produce its parent ^{99}Mo (66 h), mostly by fissioning ^{235}U with neutrons or, to a lesser extent, by the neutron bombardment of ^{98}Mo targets. After separating and purifying ^{99}Mo from the fissioned or the activated targets, it is used to prepare $^{99}\text{Mo} \rightarrow ^{99m}\text{Tc}$ generators for distribution worldwide. As of this date, no alternative method had been established to replace or as an alternative to these reactor-based techniques.

Since the early 1990's, concerns for the reliability of supply of the weekly batches of ^{99}Mo have arisen because of the age of reactors currently involved, and because of sporadic labor or technical events in some of the reactor facilities involved in its large-scale production. This concern is based on the fact that a large proportion of the current weekly supply of ^{99}Mo rely on a few reactor facilities operating in Canada and in Europe. Production of ^{99}Mo is essential for the timely manufacturing of $^{99}\text{Mo} \rightarrow ^{99m}\text{Tc}$ generators for worldwide distribution. Once on site, this device is used to elute on a daily basis, single or multiple doses of ^{99m}Tc for radiopharmaceutical syntheses. Largely due to the commitment and efficiency of the private sector operating these facilities and the distribution network, a long tradition of reliability and steady worldwide supply have been established and is expected. Over the last few years, however, some disturbances of supply have been encountered as some of the reactor facilities

have suffered from minor but potentially critical interruptions. Furthermore, because an estimated 80-90% of all the diagnostic nuclear medicine procedures performed worldwide are based on the on-site or regional preparation of ready-to-use doses of the various ^{99m}Tc radiopharmaceuticals known today, a steady supply of $^{99}\text{Mo} \rightarrow ^{99m}\text{Tc}$ generators is essential for the economic well being of the industry in general. Therefore, even a few weeks of interrupted supply may cause large economical damage as well as an interruption of clinical services. If the interruption is any longer, many medical services and health-care providers, may be seriously affected causing perhaps irreversible damage to the overall distribution and clinical use communities.

This situation could also affect many of the developing nations with nuclear medicine programs, in particular those located far away from the traditional centers of supply and distribution. Shortage of supply or limited production levels may affect their operating programs and schedules as the priority of commercial supply is usually established based upon demand and, at present, it clearly favors those large use centers located mostly in the developed nations in the northern hemisphere. Clearly, a way to alleviate this situation is to develop many alternative supply centers with capabilities for local or regional supply and based upon more affordable and reachable technologies. Accelerator programs, while still requiring major resources for implementation, and far closer than reactors in the latter category.

Preliminary investigations to develop alternative methods for producing ^{99m}Tc with accelerators were conducted in the mid 1970's. The excitation function for the production of ^{99m}Tc via the $^{100}\text{Mo}(p,2n)$ reaction in the 10 to 25 MeV proton energy region was first reported by Beaver & Hupf in 1971 [1], and was later confirmed by Almeida & Helus in 1977 [2]. However, because of the success of the $^{99}\text{Mo} \rightarrow ^{99m}\text{Tc}$ generator technique developed by Richards in 1966 [3]-no further study was reported until Lagunas-Solar et al. [4-9] developed new data over an extended proton energy range, used enriched ^{100}Mo targets, and further completed an evaluation and demonstrated the feasibility of this new accelerator-based method. The technical feasibility of using modern cyclotrons for the production of ^{99m}Tc was further analyzed by Egan et al. in 1994 [10].

Because of the above scenario, accelerator methods to provide either a direct source of ^{99m}Tc and/or of its parent ^{99}Mo are needed as potential alternatives to the reactor based production of ^{99}Mo . Therefore, also included in this study are measurements of the excitation function leading to the formation of ^{99}Mo via the $^{100}\text{Mo}(p,pn)^{99}\text{Mo}$ ($Q = - 8.3$ MeV) reaction. This latter work is a complement to other investigations regarding the use of proton-induced fission for the production of ^{99}Mo via the $^{238}\text{U}(p, \text{fission})^{99}\text{Mo}$ using accelerators [11, 12].

This report summarizes the current data base, includes a detailed accounting of experimental procedures used in this investigation, summarizes the results, and provides a discussion of the rationale behind this new accelerator-based method being developed at the University of California, Davis.

2. EXPERIMENTAL PROCEDURES

2.1. Natural Mo and enriched ^{100}Mo target materials

Natural isotopic abundance Mo, enriched ^{100}Mo (metal) and $^{98}\text{Mo}(\text{VI})$ (oxide) targets were used in all these experiments. In its metal form, Mo [$d = 10.22$ g/cm³; m.p. 2610°C; b.p. 5560°C; thermal conductivity @ 100°C 0.325 cal/(s.cm.°C)] is an excellent cyclotron target

and should be able to withstand high current bombardments. The natural and enriched $^{98}\text{Mo(VI)}$ oxide (MoO_3 , $d= 4.692 \text{ g/cm}^3$; m.p. 795°C ; b.p. 1155°C sub.) were used only in experiments conducted with low intensity beams ($< 1 \mu\text{A}$), as the Mo oxide is not an appropriate target material for high intensity bombardments. Other chemical forms of Mo were not studied as no other compound was found to have equal or better physical and chemical properties than the selected metal and oxide forms.

The isotopic composition of Mo targets that were used or considered in these experiments is given in Table I. It is specially important, in selecting the appropriate enriched ^{100}Mo target, the type and abundance of Mo isotopes present, particularly for ^{96}Mo , ^{97}Mo , and to a lesser extent for ^{98}Mo . These Mo nuclides are also targets and, therefore, are potential sources of several Tc radionuclide impurities.

The isotopic abundance of enriched ^{100}Mo from the The Commonwealth of Independent States (CIS) was selected for use in these experiments. Selection of the enriched ^{100}Mo target material was found to be a significant factor as the relative composition of the impurities from different sources is variable (Table I). The isotopic purity of ^{100}Mo is a critical factor to achieve the highest possible radionuclide purity of the directly-made $^{99\text{m}}\text{Tc}$. The rationale for this choice is discussed below (see section 3.1, Results and Discussion).

Thin natural Mo metallic foils ($12.7 \mu\text{m}$ thick, 99.95% purity, from Alfa, Johnson Matthey Company, MA) were used as single targets for the excitation function measurements. The stacked-foil technique was utilized to cover selected, narrow and broader proton energy ranges for these measurements, although, in order to check for internal consistency, a few single measurements were performed in triplicate at selected proton energies. In addition, thin natural metallic Cu foils ($12.7 \mu\text{m}$ thick, 99.8% purity, from Alfa, Johnson Matthey Company, MA) were used as secondary beam-intensity monitors. Each of the Mo and Cu foils were rectangular in shape ($3 \times 4 \text{ cm}$) and were weighted and carefully checked for thickness uniformity.

For single natural Mo targets, a Mo foil and a Cu foil were mounted together in a rectangular shaped 35-mm slide frame with the Cu foil facing the proton beam. Such arrangement guaranteed that the Cu foil would be bombarded by protons of known energy and that an essentially identical proton beam would pass through both monitor and target foils. The Cu monitor was used to confirm the total beam charge indicated by the electronic current integrator connected to a Faraday Cup. For the stacked-target experiments, three Cu foils were used: one up front of the Mo stack, one in the middle, and the third at the end of the stacked Mo foils. All three Cu foils were used as beam monitors. The entrance and exit proton energies at each Mo and Cu foils were calculated using a computer code RANGE [17], which is based on the range-energy tables given by Williamson et al. [13].

2.2. Thick enriched ^{100}Mo and ^{98}Mo targets

Enriched ^{100}Mo (97.46 % enrichment level, granular metal powder) and enriched ^{98}Mo oxide (99.45% enrichment) from CIS were used to prepare several thin ($< 1 \text{ MeV}$) and thick ($> 1 \text{ MeV}$) energy targets. The enriched ^{100}Mo targets were fabricated by pressing the powder into pellets with a diameter of 0.635 cm. Each target was enclosed within thin Cu foils which provided adequate containment in addition to serving as secondary beam monitors. Proton bombardments with up to 100 nA were conducted on a gas-cooled research target provided with the ability to determine yields and purity under various proton-energy conditions. After adequate decay periods (i.e.15-20 d), these targets were reused for further measurements. A

similar enriched ^{100}Mo thick target was also used with up to $1\ \mu\text{A}$ proton beams for yield and radiochemistry experiments (see section 2.6, below). Enriched ^{98}Mo oxide targets were prepared using similar techniques and used to test the existence of the $^{98}\text{Mo}(p,\gamma)^{99\text{m}}\text{Tc}$ reaction channel which had been predicted earlier [6].

TABLE I. ISOTOPIC ABUNDANCE OF NATURAL AND ENRICHED Mo TARGETS

Mo Isotope	Natural Mo (%)	Enriched ^{98}Mo (%)	Enriched ^{100}Mo (%) CIS (Russia) ¹	ORNL (USA)
92	14.84	0.02	0.0011	0.55
94	9.25	0.02	0.0008	0.19
95	15.92	0.04	0.0016	0.29
6	16.98	0.06	0.0020	0.35
97	9.55	0.32	0.0026	0.26
98	24.13	99.45	2.54	0.97
100	9.63	0.09	97.46	97.39

2.3. Target irradiation and proton beam monitoring

All the target irradiation were conducted with external proton beams from the 76-inch (1.93 m) isochronous cyclotron at the Crocker Nuclear Laboratory of the University of California, Davis.

All the targets, both single and stacked, natural and enriched, were irradiated under vacuum using a 76-cm diameter scattering chamber (ORTEC 2800 Series, Oak Ridge, TN) insulated electrically from a collimated beam port. An alignment of the beam collimators and the target was well established by means of a laser source prior to each experiment, and the reproducibility of this alignment was verified by video observations during irradiation. The beam size in all irradiation experiments was 0.32 cm in diameter. The proton beam charge was collected in a Faraday Cup fitted with magnetic electron suppression. In addition to the Faraday Cup, beam charge integration was also measured and checked using the $^{63}\text{Cu}(p,2n)^{62}\text{Zn}$ reaction induced in the Cu monitor foils [14]. In doing so, two characteristic γ -rays of ^{62}Zn , namely 548.4 keV (14.6%) and 596.7 keV (24.0%) were identified, measured, and used for calibrating beam intensity and for measuring the total charge of protons deposited on the targets.

The incident proton energy was measured using a time-of-flight (TOF) technique known as a γ -flash measurement [15,16]. This method essentially counts the time needed for a proton to travel between two fixed objects, a C stop and a Pb plug, separated 2.0 m apart.

2.4. Radionuclide assays

Each Mo target used in this study was assayed at least twice after irradiation. The first radioassay was conducted and completed within a few hours after the end-of-bombardment

¹ Values reported by ICP measurements.

(EOB). The cumulative activities of directly-made ^{99m}Tc , of indirectly-made ^{99m}Tc (i.e. from the decay of ^{99}Mo), and of directly-made ^{99}Mo were obtained by assaying the 140.5 keV γ -ray. After a 7-day period to allow for the decay of directly-produced ^{99m}Tc , and of other short-lived radionuclides, a second radioassay was performed to measure directly-produced ^{99}Mo , the longer-lived 66 h parent. The activity of directly-made ^{99m}Tc was then determined by analyzing the radioassays in combination, and correcting to EOB. The activity data obtained in this manner was also tested with half-life determinations. A list of radionuclides identified and measured in this work, as well as the decay data used in their respective radioassays, is given in Table II. Several other Tc isotopes were also identified and analyzed by assaying their respective γ -rays. The radioassays of the Cu monitor foils were conducted 1-day after EOB.

The first radioassay measurements were carried out with a high count rate and, therefore, were conducted using a small 0.5-cm³ high-purity Ge-detector system (Nuclear Data ND-66 MCA). A 60-Hz pulser was counted simultaneously with the Mo foils to correct for dead time and pile-up losses. All remaining radioassays were conducted at a much lower count rate and, therefore, in order to increase statistical accuracy, they were performed using a much larger, higher efficiency 20-cm³ high-purity coaxial Ge detector. These two Ge detectors were intercalibrated for absolute and relative efficiencies with a mixed-radionuclide point-source standard (National Institute of Standards and Technology, 1988).

2.5. Cross sections, yields, and uncertainties

All measured activities in counts per second (cps) from the assays were converted to cross sections and yields at EOB using the well-known activation formula. Then, the measured yields from natural Mo foils were extrapolated to enriched ^{100}Mo (CIS; 97.46 %) based upon the known isotopic compositions (Table I). The uncertainties in the cross section and yield measurements for the thin natural Mo foils amounted to $\pm 13\%$ and were estimated by combining in quadrature the individual errors listed below:

- beam-current integration ($\pm 5\%$);
- target thickness variation ($\pm 4\%$);
- spectral integration ($\pm 4\%$);
- counting statistics ($\pm 3\%$);
- detector efficiencies ($\pm 5\%$);
- attenuation corrections ($\pm 5\%$);
- γ -ray abundance ($\pm 5\%$); and
- counting geometry ($\pm 5\%$).

The uncertainties in the proton energy determinations were estimated to be $\pm 6\%$, and included in quadrature the following individual errors:

- incident beam energy ($\pm 3\%$);
- target thickness variation ($\pm 4\%$);
- beam scattering ($\pm 1\%$); and
- range energy values ($\pm 3\%$).

TABLE II. NUCLEAR AND DECAY DATA FOR TECHNETIUM ISOTOPES¹

Radionuclide	Half life	Principal γ -ray Emissions (keV, % abundance)	Decay Product
⁹³ Tc	2.75 h	1363 (66)	⁹³ Mo (3.5 x 10 ³ a)
⁹⁴ Tc	4.88 h	871 (100) 702.6 (99.8) 849.7 (96.9)	⁹⁴ Mo (Stable)
⁹⁵ Tc	20.0 h	765.8 (93)	⁹⁵ Mo (stable)
⁹⁶ Tc	4.35 d	812.5 (81.5) 849.9 (96.9)	⁹⁶ Mo (stable)
⁹⁹ Tc	2.14 x 10 ⁵ a	β^- decay	⁹⁹ Ru (stable)
^{99m} Tc	6.02 h	140.5 (89)	⁹⁹ Tc (2.14 x 10 ⁵ a)

The uncertainties in the yield measurements for the enriched ¹⁰⁰Mo thick targets were estimated to be $\pm 16\%$. The increased level of uncertainty was due to the accumulated error in the thick-target thickness which was approximately 11 times the thickness of the single thin Mo foil targets. In all the measurements of ^{99m}Tc thick-target yields, the sources of error remained the same and at levels similar to those given above.

2.6. Technetium-99m production tests with enriched ¹⁰⁰Mo and ⁹⁸Mo targets

The enriched ¹⁰⁰Mo targets were bombarded with 22.4 MeV protons (1 μ A) in a dedicated water-cooled target coupled to an external beam-line for radioisotope production at Crocker Nuclear Laboratory. After irradiation, the target was inspected for integrity, and a series of radiochemistry procedures were performed to dissolve the enriched ¹⁰⁰Mo target in 30% H₂O₂ (3 min), followed by a radiochemical separation of ^{99m}Tc radioactivities from Mo using a solvent (methyl ethyl ketone, MEK) extraction technique (< 20 min). After evaporating the organic solvent, isotonic saline was used to dissolve the ^{99m}Tc. This final ^{99m}Tc was radioassayed and the ^{99m}Tc yield and purity were compared with predicted values by extrapolation from excitation function data. The agreement between predicted and measured yield and purity values was excellent ($\pm 12\%$) providing assurances of the precision of the excitation functions obtained in this work. Similarly, experiments were conducted with protons (20-22 MeV) on enriched ⁹⁸Mo targets. After the end-of-bombardment, the target was radioassayed and no radiochemistry was performed as the results indicated extremely low production yields for ^{99m}Tc. In this manner, the predicted ⁹⁸Mo(p, γ) contribution to the ^{99m}Tc yields was tested.

3. RESULTS AND DISCUSSION

3.1. Proton-induced nuclear reactions on Mo targets

Several proton-induced nuclear reactions on Mo targets are possible in the 25-10 MeV energy region covered in this investigation. These reactions are summarized in Table III. For

¹ From "Table of Isotopes" (7th. Ed.). C.M. Lederer and V.S. Shirley (Eds.) John Wiley & Sons (1978).

TABLE III. REACTION CHANNELS FOR ≤ 25 MEV PROTONS ON ENRICHED MOLYBDENUM-100 TARGETS (CIS, ORNL)

Enriched ^{100}Mo Target (Abundance in %)	Target		Reaction for Production of $^{99\text{m}},^{96},^{95},^{94}\text{Tc}$ and ^{99}Mo Isotopes					
	CIS	ORNL	$^{99\text{m}}\text{Tc}$ (6.02 h)	^{96}Tc (4.35 d)	^{95}Tc (20.0 h)	^{94}Tc (20.0 h)	^{99}Mo (4.88 h)	^{99}Mo (66.02 h)
^{92}Mo	0.0011	0.55	n/a ²	n/a	n/a	n/a	n/a	n/a
^{94}Mo	0.0008	0.19					(p,n) Q=-5.0	
^{95}Mo	0.0016	0.29				(p,n) Q=-2.5	(p,2n) Q=-12.4	
^{96}Mo	0.0020	0.35		(p,n) Q=-3.7	(p,2n) Q=-11.6	(p,3n) Q=-21.6		
^{97}Mo	0.0026	0.26		(p,2n) Q=-10.5	(p,3n) Q=-18.5			
^{98}Mo	2.54	0.97		(p,3n) Q=-19.2				
^{100}Mo	97.46	97.39	(p,2n) Q=-7.9	n/a				(p,pn) Q=-8.3

each reaction, energetic requirement (Q-value), cross sections, and the isotopic abundance of each Mo target nuclide from which they are produced, determined the overall contribution to the yield of each specific Tc isotope. The physical properties of the Tc isotopes produced from Mo targets were already given in Table II. These properties, when analyzed in combination, provided a clear criteria of their relative significance as potential sources of Tc impurities in directly-made $^{99\text{m}}\text{Tc}$.

Although other Nb, Zr, and Y isotopes are also formed by (p,x) reactions [6], their formation and presence in an irradiated Mo target is not significant as they are effectively separated from Tc radioactivity during target radiochemistry.

Reactions leading to the formation of ^{96}Tc (4.35 d), ^{95}Tc (20.0 h) and ^{94}Tc (4.88 h) are particularly important for the production of high radionuclidic purity $^{99\text{m}}\text{Tc}$ from enriched ^{100}Mo targets. These Tc isotopes, as well as the desired $^{99\text{m}}\text{Tc}$, are produced from several Mo impurities present in enriched ^{100}Mo target materials. Therefore, the proper selection of adequately enriched ^{100}Mo is a critical choice, as there are significant differences in the isotopic abundance from the various sources considered in this study (CIS in Russia, and ORNL in the USA). The CIS material was selected, and the decision can be rationalized when inspecting the isotopic composition of ^{100}Mo enriched materials given in Table I, and analyzing it with the proton induced reactions on ^{100}Mo targets producing Tc isotopes, given in Table III.

Clearly, the production of ^{96}Tc , ^{95}Tc , and ^{94}Tc is energetically feasible within the same region of interest for the production of $^{99\text{m}}\text{Tc}$, that is, in the 25-10 MeV energy region studied. Therefore, the production of these Tc impurities must be avoided or minimized by properly selecting the enriched ^{100}Mo target material, and matching its thickness with the selected proton energy region. In order to accomplish this task, several excitation functions were measured and are reported below (see section 3.2). On the other hand, the presence of ^{98}Mo ,

¹ Reaction Q values in MeV

² Reactions not energetically possible (n/a)

^{97}Mo , ^{96}Mo , ^{95}Mo and ^{94}Mo as target nuclides in the enriched ^{100}Mo targets, was minimized by using a CIS-type rather than the ORNL-type material (Table I), simply because the CIS enriched ^{100}Mo target material had a total of 0.0070% for the combined isotopic composition of these Mo isotopes, as compared to 1.0900% for the ORNL material (a ratio of 1:156).

Among the Tc impurities observed in this investigation, ^{96}Tc (4.35 d) was clearly the main concern. The production of ^{96}Tc from these same Mo isotopic impurities (Table II) and primarily from the more abundant ^{98}Mo via the $^{98}\text{Mo}(p,3n)$ reaction ($Q = -19.2$ MeV), can be minimized by limiting the entrance proton energy on the target to ≤ 23 MeV (see section 3.4, below), a proton energy slightly above the energetic threshold for the $^{98}\text{Mo}(p,3n)$ reaction. The results of this strategy and a discussion of the many possible options regarding target material and operating proton energy ranges, is given below.

3.2. Excitation functions for the $\text{Mo}(p,xn)\text{Tc}$ reactions

Previously reported excitation functions for the proton-induced reactions on natural Mo targets [6] suggested the possibility that two reaction channels, a lower energy $^{98}\text{Mo}(p,\gamma)$ and a higher energy $^{100}\text{Mo}(p,2n)$, were available for the production of ^{99m}Tc in the 70 to 10 MeV region. However, this interpretation of the empirical data obtained by assaying the typical 140.5-keV γ -ray emission from the 6.02 ^{99m}Tc , was proved as incorrect when it was compared with data obtained in this study with enriched ^{100}Mo targets. The consecutive long-term assays (over 7-10 days after EOB) of the 140.5 keV region taken from the different natural Mo targets used in the previous work, had to be corrected from several potential interference including similar γ -ray emissions from ^{99}Mo (140 keV, 88.7%) and its daughter ^{99m}Tc , to obtain the true count rate for the directly-made ^{99m}Tc . These time-dependent corrections allowed the determination of the true count rate for directly-made ^{99m}Tc by correcting the total count rate for the 140.5 keV region being assayed over time. Although corrections were made to account for the presence of other interfering γ -ray emissions, particularly from the 141-keV (61%) γ ray from ^{90}Nb (14.8 h), it appears that some nuclear decay data is either not correct or does not exist as the corrections produced the doubly peaked excitation function reported earlier [6,7]. In natural Mo targets, ^{90}Nb may be produced indirectly by the $^{92}\text{Mo}(14.84\%)(p,3n)^{90g,m}\text{Tc}$ (49.2 s; 8.3 s) \rightarrow ^{90}Mo (5.67 h) \rightarrow ^{90}Nb ($Q = -32.43$ MeV) and/or directly by the $^{94}\text{Mo}(9.25\%)(p,\alpha n)^{90}\text{Nb}$ reaction ($Q = -8.97$ MeV). Clearly, the presence of ^{90}Nb and/or an unknown contaminant dominated adversely the intended corrections for the “true count rate” due to the directly-made ^{99m}Tc .

In addition, we also used CIS enriched ^{98}Mo targets (Table I) to test the potential of the $^{98}\text{Mo}(p,\gamma)$ contribution, and limited our observations to below 25 MeV. In this manner, the suspected contribution of the (p, γ) reaction channel was discarded as small cross sections were predicted based on extremely low measured ^{99m}Tc yields (data not shown). Therefore, the interpretation advanced previously [6] on the double “hump” excitation function was proven incorrect and discarded.

The excitation functions measured are summarized in Table IV, and shown in Fig. 1 for ^{99m}Tc ; Fig. 2 for ^{96}Tc ; Fig. 3 for ^{95}Tc ; and Fig. 4 for ^{94}Tc . Because of reaction energetic, target isotopic composition, and proton beam energies, only the ^{99m}Tc cross section data was clearly identified as a single $^{100}\text{Mo}(p,2n)$ reaction channel, and is reported as such. In all other cases, the production of Tc isotopes results from an integration of several reaction channels which are energetically feasible and, thus, allowed in the proton energy range studied and because of the presence of diverse Mo target nuclides being bombarded. The proton energy assigned to

each thin Mo target was calculated as the mean between incident and exit energies. Exit energies were calculated using a computer code RANGE [17] and the corresponding target thickness.

This calculation procedure was employed with all targets, including both single and stacked, natural and enriched, Mo targets and Cu monitor foils, used in this investigation. In addition, the excitation function for the production of ^{99}Mo via the $^{100}\text{Mo}(p,pn)^{99}\text{Mo}$ reaction ($Q = -8.3$ MeV) is also given in Table IV, and will be discussed in section 3.8, below.

3.2.1. Excitation function for $^{100}\text{Mo}(p,2n)^{99m}\text{Tc}$ reaction

The excitation function for the $^{100}\text{Mo}(p,2n)^{99m}\text{Tc}$ reaction was measured directly with natural Mo and is shown in Fig. 1. As the only possible contributor in a natural Mo target is the ^{100}Mo nuclide (9.63%), this data provided unequivocal information on this reaction channel. A fit curve of the excitation function for the ^{99m}Tc cross section data shown in Fig. 1, indicated a maximum cross section of 365 ± 47 mb at 16.5 MeV. This maximum cross section is slightly larger than the value of 290 mb reported earlier by Lagunas-Solar et al. [6] and than the 305 mb value reported by Levkovskii [18]. However, the proton energy at which the maximum cross section was measured in this work is in good agreement and within the experimental uncertainty with the 17-MeV maximum reported by Lagunas-Solar [6], and is slightly higher than the 14.8-MeV value reported by Levkovskii [18].

Contrary to what was suggested in previous work [6], no double “hump” excitation function resulted providing an unequivocal solution to the former prediction. The precision of this excitation function is critical for establishing the best operating parameters for ^{99m}Tc yield and purity optimization. This function is also critical in optimizing the incident proton energy and the isotopic purity of the enriched ^{100}Mo target material. To a smaller extent, the exit proton energies, determined by varying the target thickness, is a lesser factor, as the relative contribution to the ^{99m}Tc yield decreases with proton energy. On the other hand, thicker targets shall improve purity as no other Tc impurity is produced significantly, below 19 MeV. This is due to the low abundance of Mo nuclide “impurities” in the CIS ^{100}Mo target material which has 2.54% of ^{98}Mo , but only 0.0026% of ^{97}Mo and 0.0020% of ^{96}Mo , the other potential sources of ^{96}Tc (Table III). Finally, and due to the low abundance of the target Mo nuclides (i.e. ^{97}Mo [0.0026%], ^{96}Mo [0.0020%], ^{95}Mo [0.0016%] and ^{94}Mo [0.0008%]), all other potential Tc impurities such as 20.0 h ^{95}Tc and 4.88 h ^{94}Tc are produced in extremely low yields and were undetectable (below detectable levels) in several ^{99m}Tc production test runs conducted in this study (see section 3.5, below).

TABLE IV. TOTAL CROSS SECTIONS FOR THE PRODUCTION OF $^{99m,96,95,94}\text{Tc}$ AND ^{99}Mo ISOTOPES WITH PROTONS ON NATURAL Mo TARGETS.

Proton Energy (MeV)	^{99m}Tc (mb)	^{96}Tc (mb)	^{95}Tc (mb)	^{94}Tc (mb)	^{99}Mo (mb)
9.54 ± 0.57	51.8 ± 6.7	622 ± 81	123.8 ± 16.1	446 ± 58	
9.87 ± 0.59	83.3 ± 10.8	662 ± 86	212.2 ± 27.6	475 ± 62	
10.2 ± 0.6	124 ± 16	717 ± 93	302.1 ± 39.3	558 ± 73	
10.5 ± 0.6	166 ± 22	789 ± 103	387.3 ± 50.3	546 ± 71	
10.8 ± 0.6	188 ± 24	804 ± 105	553.5 ± 72.0	451 ± 59	
11.1 ± 0.7	216 ± 28	838 ± 109	569.3 ± 74.0	350 ± 46	
11.4 ± 0.7	243 ± 32	879 ± 114	610.7 ± 79.4	331 ± 43	
11.7 ± 0.7	269 ± 35	989 ± 129	588.1 ± 76.5	320 ± 42	
12.0 ± 0.7	279 ± 36	1040 ± 135	565.0 ± 73.5	384 ± 50	

TABLE IV. (Cont.)

Proton Energy (MeV)	^{99m} Tc (mb)	⁹⁶ Tc (mb)	⁹⁵ Tc (mb)	⁹⁴ Tc (mb)	⁹⁹ Mo (mb)
12.2 ± 0.7	288 ± 37	1080 ± 140	612.6 ± 79.6	340 ± 44	
12.5 ± 0.8	297 ± 39	1179 ± 153	657.7 ± 85.5	316 ± 41	
12.8 ± 0.8	303 ± 39	1309 ± 170	692.1 ± 90.0	319 ± 41	
13.0 ± 0.8	304 ± 40	1257 ± 163	661.3 ± 86.0	227 ± 30	
13.3 ± 0.8	327 ± 43	1296 ± 168	768.8 ± 99.9	254 ± 33	4.86 ± 0.63
13.5 ± 0.8	326 ± 42	1229 ± 160	760.1 ± 98.8	300 ± 39	5.83 ± 0.76
13.8 ± 0.8	338 ± 44	1226 ± 159	927 ± 121	340 ± 44	8.97 ± 1.2
14.0 ± 0.8	327 ± 43	1171 ± 152	888 ± 115	361 ± 47	10.8 ± 1.4
14.2 ± 0.9	345 ± 45	1189 ± 155	915 ± 119	380 ± 49	11.3 ± 1.5
14.2 ± 0.9	335 ± 44	1196 ± 155	963 ± 125	389 ± 51	15.3 ± 2.0
14.2 ± 0.9	335 ± 44	1201 ± 156	897 ± 117	387 ± 50	16.0 ± 2.1
14.3 ± 0.9	325 ± 42	1210 ± 157	936 ± 122	404 ± 53	15.9 ± 2.1
14.5 ± 0.9	329 ± 43	1144 ± 149	863 ± 112	431 ± 56	15.5 ± 2.0
14.6 ± 0.9	370 ± 48	1125 ± 146	834 ± 108	597 ± 78	28.8 ± 3.7
14.6 ± 0.9	379 ± 49	1128 ± 147	872 ± 113	609 ± 79	28.8 ± 3.7
14.6 ± 0.9	388 ± 50	1161 ± 151	855 ± 111	557 ± 72	26.2 ± 3.4
14.8 ± 0.9	329 ± 43	1092 ± 142	931 ± 121	563 ± 73	30.5 ± 4.0
16.0 ± 1.0	364 ± 47	1027 ± 134	983 ± 128	698 ± 91	34.9 ± 4.5
16.0 ± 1.0	351 ± 46	1014 ± 132	993 ± 129	681 ± 89	33.9 ± 4.4
16.0 ± 1.0	327 ± 43	928 ± 121	1021 ± 133	530 ± 69	33.7 ± 4.4
17.0 ± 1.0	381 ± 50	933 ± 121	956 ± 124	600 ± 78	43.8 ± 5.7
17.0 ± 1.0	362 ± 47	884 ± 115	938 ± 122	707 ± 92	44.6 ± 5.8
17.0 ± 1.0	352 ± 46	897 ± 117	989 ± 129	654 ± 85	48.9 ± 6.4
17.9 ± 1.1	346 ± 45	944 ± 123	941 ± 122	629 ± 82	49.7 ± 6.5
18.1 ± 1.1	343 ± 45	938 ± 122	910 ± 118	627 ± 82	49.9 ± 6.5
18.3 ± 1.1	340 ± 44	956 ± 124	964 ± 125	550 ± 72	54.9 ± 7.1
18.5 ± 1.1	334 ± 43	882 ± 115	906 ± 118	640 ± 83	56.9 ± 7.4
18.7 ± 1.1	330 ± 43	860 ± 112	868 ± 113	685 ± 89	59.1 ± 7.7
19.1 ± 1.1	310 ± 40	965 ± 125	1024 ± 133	634 ± 82	57.8 ± 7.5
19.2 ± 1.2	314 ± 41	861 ± 112	959 ± 125	643 ± 84	60.6 ± 7.9
19.4 ± 1.2	285 ± 37	957 ± 124	927 ± 121	609 ± 79	54.7 ± 7.1
19.6 ± 1.2	273 ± 35	901 ± 117	887 ± 115	544 ± 71	55.3 ± 7.2
19.8 ± 1.2	261 ± 34	920 ± 120	899 ± 117	511 ± 66	55.0 ± 7.2
20.2 ± 1.2	312 ± 41	921 ± 120	944 ± 123	599 ± 78	51.7 ± 6.7
20.2 ± 1.2	319 ± 41	900 ± 117	975 ± 127	725 ± 94	52.1 ± 6.8
20.2 ± 1.2	316 ± 41	910 ± 118	948 ± 123	707 ± 92	53.3 ± 6.9
20.7 ± 1.2	243 ± 32	901 ± 117	901 ± 117	487 ± 63	52.2 ± 6.8
20.9 ± 1.3	239 ± 31	884 ± 115	859 ± 112	498 ± 65	53.3 ± 6.9
21.0 ± 1.3	222 ± 29	870 ± 113	831 ± 108	551 ± 72	52.7 ± 6.9
21.2 ± 1.3	232 ± 30	857 ± 111	873 ± 113	627 ± 82	48.4 ± 6.3
21.4 ± 1.3	203 ± 26	856 ± 111	925 ± 120	489 ± 64	49.1 ± 6.4
21.6 ± 1.3	201 ± 26	877 ± 114	852 ± 111	605 ± 79	48.9 ± 6.4
22.0 ± 1.3	195 ± 25	849 ± 110	893 ± 116	516 ± 67	49.7 ± 6.5
22.1 ± 1.3	183 ± 24	869 ± 113	940 ± 122	480 ± 62	63.7 ± 8.3
22.3 ± 1.3	167 ± 22	901 ± 117	977 ± 127	603 ± 78	62.1 ± 8.1
22.3 ± 1.3	171 ± 22	1049 ± 136	1009 ± 131	650 ± 85	65.3 ± 8.5
22.4 ± 1.3	150 ± 20	1025 ± 133	1088 ± 141	619 ± 80	52.4 ± 6.8
22.4 ± 1.3	137 ± 18	1001 ± 130	1159 ± 151	622 ± 81	60.4 ± 7.9
22.4 ± 1.3	139 ± 18	1015 ± 132	1128 ± 147	643 ± 84	55.3 ± 7.2

TABLE IV. (Cont.)

Proton Energy (MeV)	^{99m}Tc (mb)	^{96}Tc (mb)	^{95}Tc (mb)	^{94}Tc (mb)	^{99}Mo (mb)
22.5 ± 1.4	189 ± 25	998 ± 130	976 ± 127	619 ± 80	60.9 ± 7.9
22.5 ± 1.4	163 ± 21	871 ± 113	907 ± 118	622 ± 81	57.3 ± 7.4
22.7 ± 1.4	168 ± 22	1042 ± 135	1092 ± 142	500 ± 65	60.3 ± 7.8
22.7 ± 1.4	151 ± 20	904 ± 118	861 ± 112	530 ± 69	55.3 ± 7.2
22.8 ± 1.4	148 ± 19	1047 ± 136	984 ± 128	605 ± 79	56.3 ± 7.3
22.8 ± 1.4	141 ± 18	968 ± 126	939 ± 122	645 ± 84	57.0 ± 7.4
23.0 ± 1.4	143 ± 19	1057 ± 137	968 ± 126	595 ± 77	59.9 ± 7.8
23.0 ± 1.4	152 ± 20	1001 ± 130	1123 ± 146	506 ± 66	60.8 ± 7.9
23.3 ± 1.4	141 ± 18	1048 ± 136	1017 ± 132	552 ± 72	58.5 ± 7.6
23.5 ± 1.4	131 ± 17	1076 ± 140	1146 ± 149	556 ± 72	61.5 ± 8.0
23.6 ± 1.4	133 ± 17	1205 ± 157	1047 ± 136	570 ± 74	64.4 ± 8.4
23.8 ± 1.4	113 ± 15	1114 ± 145	1242 ± 161	549 ± 71	64.3 ± 8.4
23.9 ± 1.4	118 ± 15	1115 ± 145	1173 ± 152	629 ± 82	65.0 ± 8.5
24.1 ± 1.4	113 ± 15	1133 ± 147	1095 ± 142	596 ± 77	64.7 ± 8.4
24.6 ± 1.5	118 ± 15	1253 ± 163	1252 ± 163	667 ± 87	65.8 ± 8.6
24.6 ± 1.5	124 ± 16	1215 ± 158	1204 ± 157	662 ± 86	67.5 ± 8.8
24.6 ± 1.5	120 ± 16	1235 ± 161	1235 ± 161	654 ± 85	65.4 ± 8.5

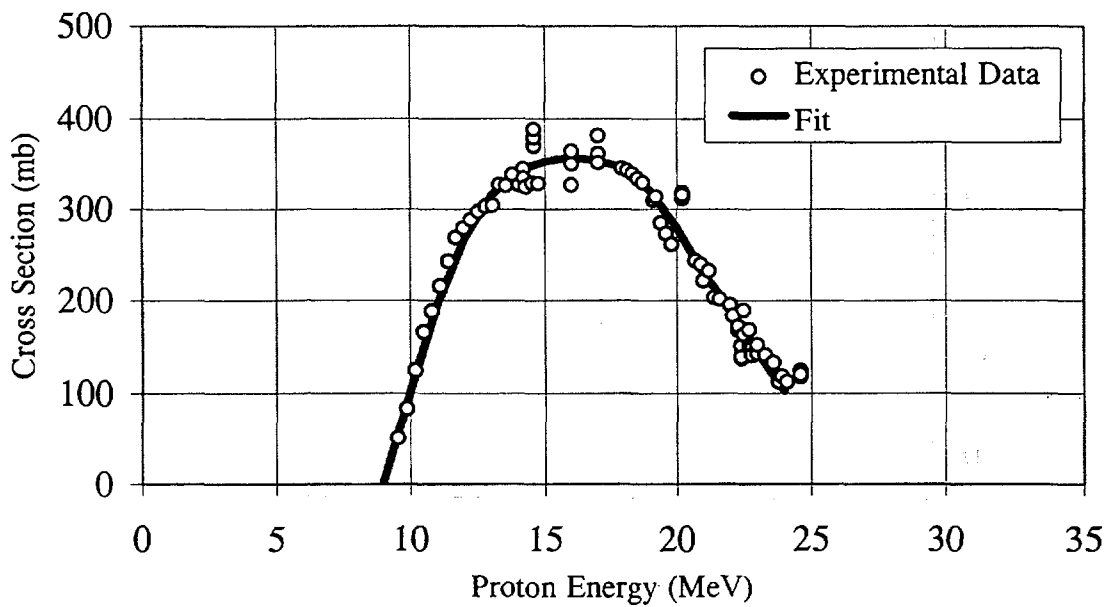


FIG. 1. Excitation function for the $^{100}\text{Mo}(p,2n)^{99m}\text{Tc}$ reaction ($Q = -7.9$ MeV).

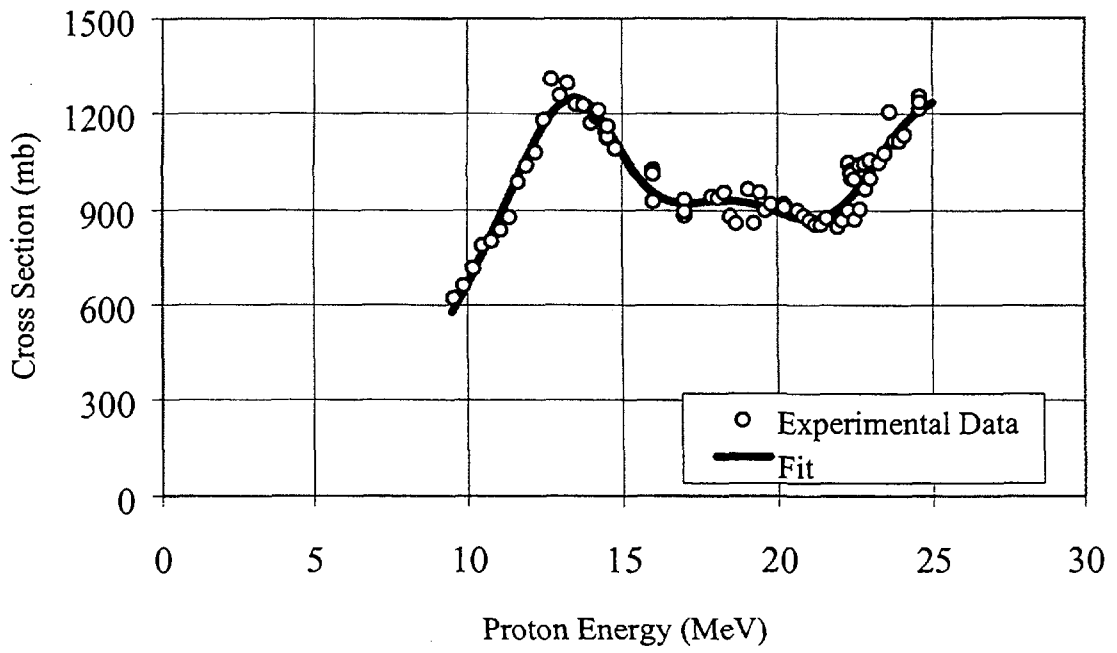


FIG. 2. Excitation function for the $^{nat}\text{Mo}(p,xn)^{96}\text{Tc}$ reaction.

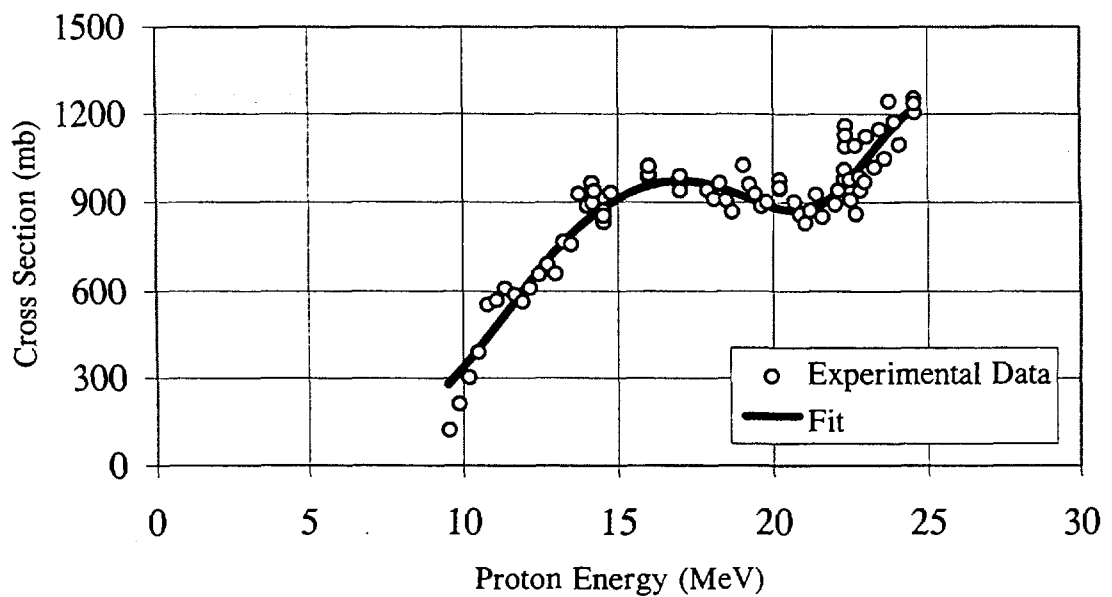


FIG. 3. Excitation function for the $^{nat}\text{Mo}(p,xn)^{95}\text{Tc}$ reaction.

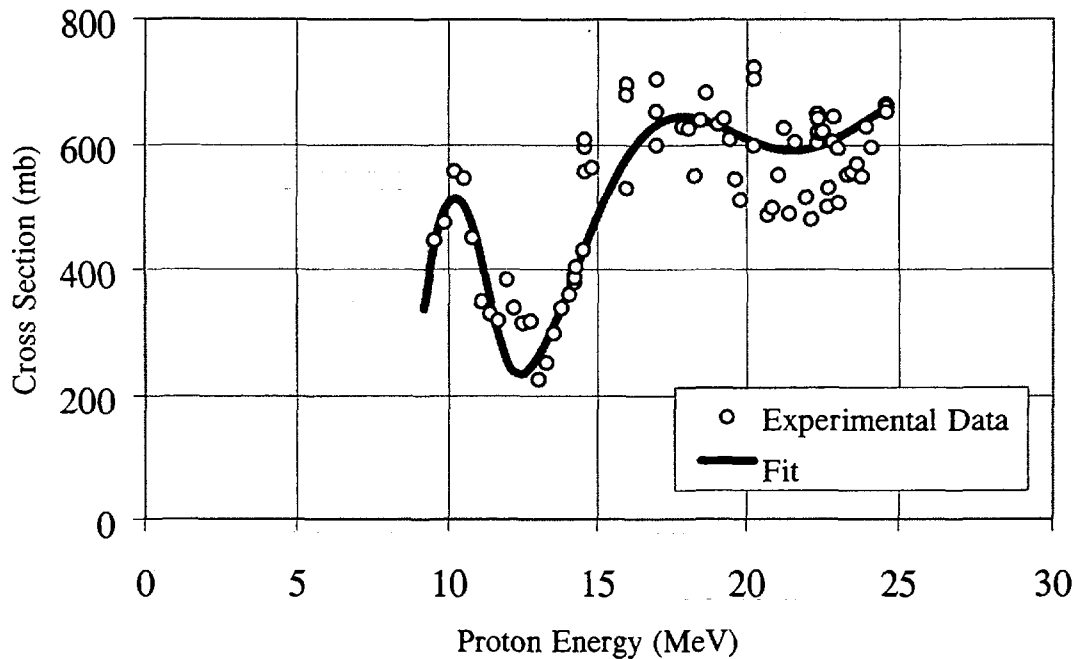


FIG. 4. Excitation function for the $^{nat}\text{Mo}(p,xn)^{94}\text{Tc}$ reaction.

3.2.2. Excitation functions for $^{nat}\text{Mo}(p,xn)^{96,95,94}\text{Tc}$ reactions

The excitation functions measured for the $^{nat}\text{Mo}(p,xn)^{96,95,94}\text{Tc}$ reactions provided with information on the total cross sections for the production of these Tc isotopes as the total activities induced resulted from contributions of several Mo nuclides present in the target (Table II).

In order to get the contribution of individual reaction channels to the production of any of the predicted Tc (^{96}Tc , ^{95}Tc , ^{94}Tc) impurities, the excitation functions given in Table IV were unfolded using the guidance provided by nuclear reaction systematic, reaction energetic, and knowing the isotopic composition of both enriched (CIS) ^{100}Mo and natural Mo target materials. These individual contributions are needed to be able to extrapolate to the isotopic composition of any enriched ^{100}Mo target material considered for this accelerator-based method, and to be able to extrapolate to any of the yields for the $^{96,95,94}\text{Tc}$ impurities.

3.3. Yield estimates with enriched ^{100}Mo (CIS; 97.46%)

The ^{99m}Tc , ^{96}Tc , ^{95}Tc , and ^{94}Tc yields for enriched ^{100}Mo (CIS; 97.46%) targets are given in Table V, and shown in Figures 5-8, respectively. The conversion of cross section data to yield values was direct and straightforward for ^{99m}Tc , as both excitation and the yield functions are identical in shape and boundaries. As expected from the excitation function shown in Fig. 1, the large ^{99m}Tc yield vs. energy function shown in Fig.5, peaked at 16.5 MeV. This yield data also demonstrated that the direct production of ^{99m}Tc in large batches is possible using < 25 MeV protons and enriched ^{100}Mo targets. Integration of the yield data in any selected energy regions allows for the evaluation of yield and purity for all the Tc isotopes of concern, using a variety of proton beam (energy, intensity) and target (thickness, isotopic purity) conditions. Examples of these calculations are given and discussed below.

However, the precision of the yield estimates for ^{96}Tc , ^{95}Tc , and ^{94}Tc , produced by the unfolding method, needed further testing (see section 3.4, below). Further analysis of the yield data to evaluate the potential for the production of Tc impurities (see Figures 6, 7, 8), clearly indicated that the incident proton beam energy should be kept below 23 MeV. There is no limitation regarding purity with respect to exit proton energies. However, as target thickness increases, other concerns regarding target power deposition and its operational reliability, would increase if high intensity proton bombardments are considered.

3.4. Comparison of theoretical and experimental yield and purity values

In order to test the validity of the cross section and yield data summarized above, especially its extrapolation to thick target conditions, several low-intensity production tests were conducted with the enriched ^{100}Mo (CIS; 97.46%) target material. Single targets were bombarded with 20.5 ± 0.1 MeV protons at 100 nA for approximately 10 minutes, using the scattering chamber setup (see section 2.3). The targets were radioassayed immediately and after a decay period, but no radiochemical separations were attempted. The results of these measurements are given in Table VI.

The measured yield and purity for each test compared well-within the levels of the total uncertainty-with extrapolated values obtained from the excitation function data. The proton energy for each ^{100}Mo target was calculated and is reported as the mean value between the

TABLE V. EXTRAPOLATED Tc YIELDS FROM ENRICHED ^{100}Mo (CIS; (97.46%))

Target Energy (MeV)	^{99m}Tc (mCi/ $\mu\text{Ah}/\text{MeV}$)	^{96}Tc ($\mu\text{Ci}/\mu\text{Ah}/\text{MeV}$)	^{95}Tc ($\mu\text{Ci}/\mu\text{Ah}/\text{MeV}$)	^{94}Tc ($\mu\text{Ci}/\mu\text{Ah}/\text{MeV}$)
9.54 \pm 0.57	0.244 \pm 0.032	0.00350 \pm 0.00046	0.00010 \pm 0.00001	0.0228 \pm 0.0030
9.87 \pm 0.59	0.403 \pm 0.052	0.00382 \pm 0.00050	0.00030 \pm 0.00004	0.0220 \pm 0.0029
10.2 \pm 0.6	0.615 \pm 0.080	0.00420 \pm 0.00055	0.00307 \pm 0.00040	0.0282 \pm 0.0037
10.5 \pm 0.6	0.83 \pm 0.11	0.00465 \pm 0.00060	0.0098 \pm 0.0013	0.0282 \pm 0.0037
10.8 \pm 0.6	0.97 \pm 0.13	0.00479 \pm 0.00062	0.0143 \pm 0.0019	0.0237 \pm 0.0031
11.1 \pm 0.7	1.15 \pm 0.15	0.00506 \pm 0.00066	0.0150 \pm 0.0020	0.0185 \pm 0.0024
11.4 \pm 0.7	1.29 \pm 0.17	0.00536 \pm 0.00070	0.0165 \pm 0.0021	0.0223 \pm 0.0029
11.7 \pm 0.7	1.48 \pm 0.19	0.00602 \pm 0.00078	0.0219 \pm 0.0028	0.0179 \pm 0.0023
12.0 \pm 0.7	1.54 \pm 0.20	0.00640 \pm 0.00083	0.0159 \pm 0.0021	0.0218 \pm 0.0028
12.2 \pm 0.7	1.65 \pm 0.21	0.00677 \pm 0.00088	0.0210 \pm 0.0027	0.0125 \pm 0.0016
12.5 \pm 0.8	1.70 \pm 0.22	0.00733 \pm 0.00095	0.0185 \pm 0.0024	0.0244 \pm 0.0032
12.8 \pm 0.8	2.13 \pm 0.28	0.0080 \pm 0.0010	0.0205 \pm 0.0027	0.0198 \pm 0.0026
13.0 \pm 0.8	1.81 \pm 0.24	0.0077 \pm 0.0010	0.0199 \pm 0.0026	0.0252 \pm 0.0033
13.3 \pm 0.8	2.03 \pm 0.26	0.0080 \pm 0.0010	0.0236 \pm 0.0031	0.0271 \pm 0.0035
13.5 \pm 0.8	2.02 \pm 0.26	0.00761 \pm 0.00099	0.0236 \pm 0.0031	0.0309 \pm 0.0040
13.8 \pm 0.8	2.09 \pm 0.27	0.00759 \pm 0.00099	0.0293 \pm 0.0038	0.0348 \pm 0.0046
14.0 \pm 0.8	2.02 \pm 0.26	0.00720 \pm 0.00094	0.0285 \pm 0.0037	0.0369 \pm 0.0048
14.2 \pm 0.9	2.16 \pm 0.28	0.0079 \pm 0.0010	0.0293 \pm 0.0038	0.0384 \pm 0.0050
14.2 \pm 0.9	1.97 \pm 0.26	0.0083 \pm 0.0011	0.0297 \pm 0.0039	0.0406 \pm 0.0053
14.2 \pm 0.9	2.16 \pm 0.28	0.0084 \pm 0.0011	0.0312 \pm 0.0041	0.0427 \pm 0.0056
14.3 \pm 0.9	2.09 \pm 0.27	0.00739 \pm 0.00096	0.0305 \pm 0.0040	0.0421 \pm 0.0055
14.5 \pm 0.9	2.12 \pm 0.28	0.00692 \pm 0.00090	0.0285 \pm 0.0037	0.0462 \pm 0.0060
14.6 \pm 0.9	2.58 \pm 0.34	0.00719 \pm 0.00093	0.0281 \pm 0.0037	0.0501 \pm 0.0065
14.6 \pm 0.9	2.46 \pm 0.32	0.00715 \pm 0.00093	0.0293 \pm 0.0038	0.0598 \pm 0.0078
14.6 \pm 0.9	2.52 \pm 0.33	0.00717 \pm 0.00093	0.0287 \pm 0.0037	0.0699 \pm 0.0091
14.8 \pm 0.9	2.12 \pm 0.28	0.00698 \pm 0.00091	0.0299 \pm 0.0039	0.0481 \pm 0.0063

TABLE V. (Cont.)

Target Energy (MeV)	^{99m}Tc (mCi/ $\mu\text{Ah}/\text{MeV}$)	^{96}Tc ($\mu\text{Ci}/\mu\text{Ah}/\text{MeV}$)	^{95}Tc ($\mu\text{Ci}/\mu\text{Ah}/\text{MeV}$)	^{94}Tc ($\mu\text{Ci}/\mu\text{Ah}/\text{MeV}$)
16.0 \pm 1.0	2.76 \pm 0.36	0.0078 \pm 0.0010	0.0363 \pm 0.0047	0.0649 \pm 0.0084
16.0 \pm 1.0	2.66 \pm 0.35	0.0077 \pm 0.0010	0.0359 \pm 0.0047	0.0701 \pm 0.0091
16.0 \pm 1.0	2.48 \pm 0.32	0.00710 \pm 0.00092	0.0373 \pm 0.0048	0.0545 \pm 0.0071
17.0 \pm 1.0	2.88 \pm 0.37	0.00705 \pm 0.00092	0.0365 \pm 0.0047	0.0543 \pm 0.0071
17.0 \pm 1.0	2.73 \pm 0.35	0.00705 \pm 0.00092	0.0359 \pm 0.0047	0.0671 \pm 0.0087
17.0 \pm 1.0	2.66 \pm 0.35	0.00699 \pm 0.00091	0.0378 \pm 0.0049	0.079 \pm 0.010
17.9 \pm 1.1	2.67 \pm 0.35	0.00668 \pm 0.00087	0.0375 \pm 0.0049	0.0759 \pm 0.0099
18.1 \pm 1.1	2.68 \pm 0.35	0.00668 \pm 0.00087	0.0366 \pm 0.0048	0.078 \pm 0.010
18.3 \pm 1.1	2.67 \pm 0.35	0.00684 \pm 0.00089	0.0392 \pm 0.0051	0.0696 \pm 0.0090
18.5 \pm 1.1	2.65 \pm 0.34	0.00687 \pm 0.00089	0.0371 \pm 0.0048	0.082 \pm 0.011
18.7 \pm 1.1	2.64 \pm 0.34	0.00686 \pm 0.00089	0.0359 \pm 0.0047	0.089 \pm 0.012
19.1 \pm 1.1	2.52 \pm 0.33	0.00689 \pm 0.00090	0.0430 \pm 0.0056	0.084 \pm 0.011
19.4 \pm 1.2	2.35 \pm 0.31	0.00704 \pm 0.00092	0.0393 \pm 0.0051	0.082 \pm 0.0011
19.8 \pm 1.2	2.18 \pm 0.28	0.00697 \pm 0.00091	0.0388 \pm 0.0050	0.0705 \pm 0.0092
20.2 \pm 1.2	2.71 \pm 0.35	0.00750 \pm 0.00098	0.0414 \pm 0.0054	0.104 \pm 0.014
20.2 \pm 1.2	2.65 \pm 0.34	0.0085 \pm 0.0011	0.0427 \pm 0.0056	0.126 \pm 0.016
20.2 \pm 1.2	2.68 \pm 0.35	0.0095 \pm 0.0012	0.0416 \pm 0.0054	0.123 \pm 0.016
20.7 \pm 1.2	2.05 \pm 0.27	0.0105 \pm 0.0014	0.0377 \pm 0.0049	0.0747 \pm 0.0097
20.9 \pm 1.3	2.03 \pm 0.26	0.0120 \pm 0.0016	0.0448 \pm 0.0058	0.080 \pm 0.010
21.0 \pm 1.3	1.89 \pm 0.25	0.0125 \pm 0.0016	0.0434 \pm 0.0056	0.089 \pm 0.012
21.2 \pm 1.3	2.00 \pm 0.26	0.0130 \pm 0.0017	0.0415 \pm 0.0054	0.103V 0.013
21.4 \pm 1.3	1.76 \pm 0.23	0.0133 \pm 0.0017	0.0488 \pm 0.0063	0.081 \pm 0.011
21.6 \pm 1.3	1.75 \pm 0.23	0.0138 \pm 0.0018	0.0452 \pm 0.0059	0.090 \pm 0.012
22.0 \pm 1.3	1.72 \pm 0.22	0.0138 \pm 0.0018	0.0450 \pm 0.0059	0.078 \pm 0.010
22.1 \pm 1.3	1.62 \pm 0.21	0.0145 \pm 0.0019	0.0498 \pm 0.0065	0.0732 \pm 0.0095
22.3 \pm 1.3	1.49 \pm 0.19	0.0148 \pm 0.0019	0.0521 \pm 0.0068	0.093 \pm 0.011
22.3 \pm 1.3	1.59 \pm 0.21	0.0172 \pm 0.0022	0.0538 \pm 0.0070	0.099 \pm 0.013
22.4 \pm 1.3	1.38 \pm 0.18	0.0179 \pm 0.0023	0.0580 \pm 0.0075	0.095 \pm 0.012
22.4 \pm 1.3	1.25 \pm 0.16	0.0175 \pm 0.0023	0.0618 \pm 0.0080	0.095 \pm 0.012
22.4 \pm 1.3	1.27 \pm 0.17	0.0171 \pm 0.0022	0.0601 \pm 0.0078	0.099 \pm 0.013
22.5 \pm 1.4	1.68 \pm 0.22	0.0177 \pm 0.0023	0.0513 \pm 0.0067	0.095 \pm 0.012
22.5 \pm 1.4	1.52 \pm 0.20	0.0155 \pm 0.0020	0.0477 \pm 0.0062	0.0520 \pm 0.0068
22.7 \pm 1.4	1.42 \pm 0.18	0.0186 \pm 0.0024	0.0571 \pm 0.0074	0.078 \pm 0.010
22.7 \pm 1.4	1.52 \pm 0.20	0.0161 \pm 0.0021	0.0451 \pm 0.0059	0.083 \pm 0.011
22.8 \pm 1.4	1.34 \pm 0.17	0.0193 \pm 0.0025	0.0516 \pm 0.0067	0.095 \pm 0.012
22.8 \pm 1.4	1.33 \pm 0.17	0.0164 \pm 0.0021	0.0492 \pm 0.0064	0.101 \pm 0.013
23.0 \pm 1.4	1.44 \pm 0.19	0.0199 \pm 0.0026	0.0510 \pm 0.0066	0.094 \pm 0.012
23.0 \pm 1.4	1.31 \pm 0.17	0.0170 \pm 0.0022	0.0591 \pm 0.0077	0.080 \pm 0.010
23.3 \pm 1.4	1.34 \pm 0.17	0.0205 \pm 0.0027	0.0535 \pm 0.0070	0.088 \pm 0.011
23.5 \pm 1.4	1.26 \pm 0.16	0.0217 \pm 0.0028	0.0598 \pm 0.0078	0.089 \pm 0.012
23.6 \pm 1.4	1.29 \pm 0.17	0.0244 \pm 0.0032	0.0548 \pm 0.0071	0.091 \pm 0.012
23.8 \pm 1.4	1.09 \pm 0.14	0.0232 \pm 0.0030	0.0650 \pm 0.0085	0.089 \pm 0.012
23.9 \pm 1.4	1.16 \pm 0.15	0.0238 \pm 0.0031	0.0645 \pm 0.0084	0.102 \pm 0.013
24.1 \pm 1.4	1.11 \pm 0.14	0.0244 \pm 0.0032	0.0576 \pm 0.0075	0.098 \pm 0.013
24.6 \pm 1.5	1.17 \pm 0.15	0.0242 \pm 0.0031	0.0705 \pm 0.0092	0.113V 0.015
24.6 \pm 1.5	1.15 \pm 0.15	0.0242 \pm 0.0031	0.0732 \pm 0.0095	0.109 \pm 0.014
24.6 \pm 1.5	1.21 \pm 0.16	0.0242 \pm 0.0031	0.0703 \pm 0.0091	0.107 \pm 0.014

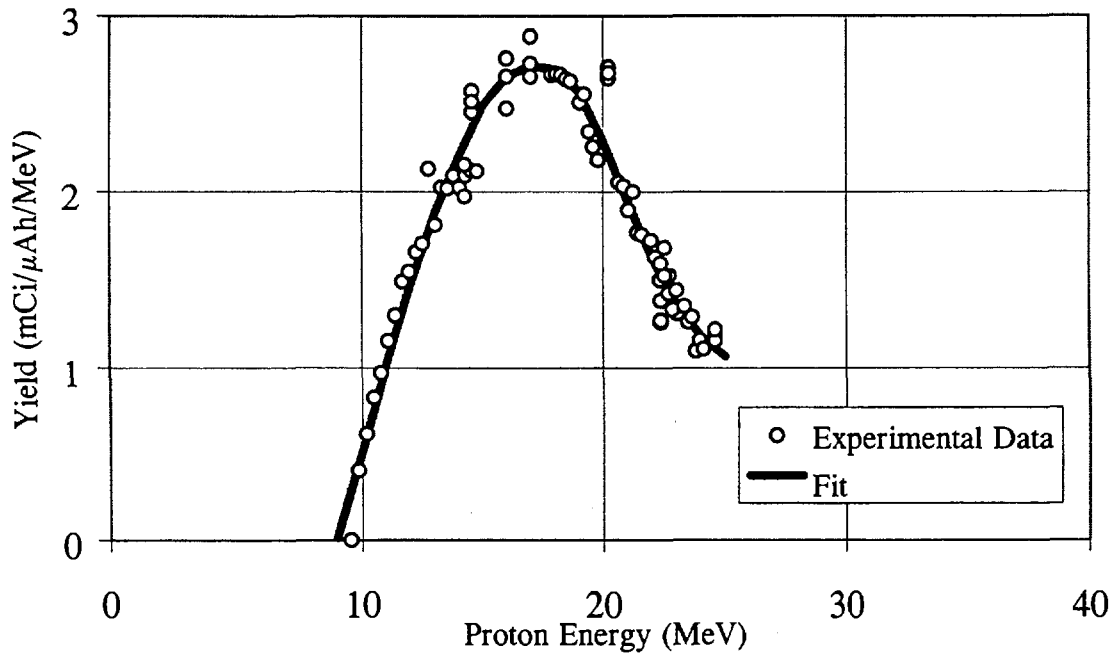


FIG. 5. Extrapolated ^{99m}Tc yields to enriched ^{100}Mo (CIS; 97.46%) targets.

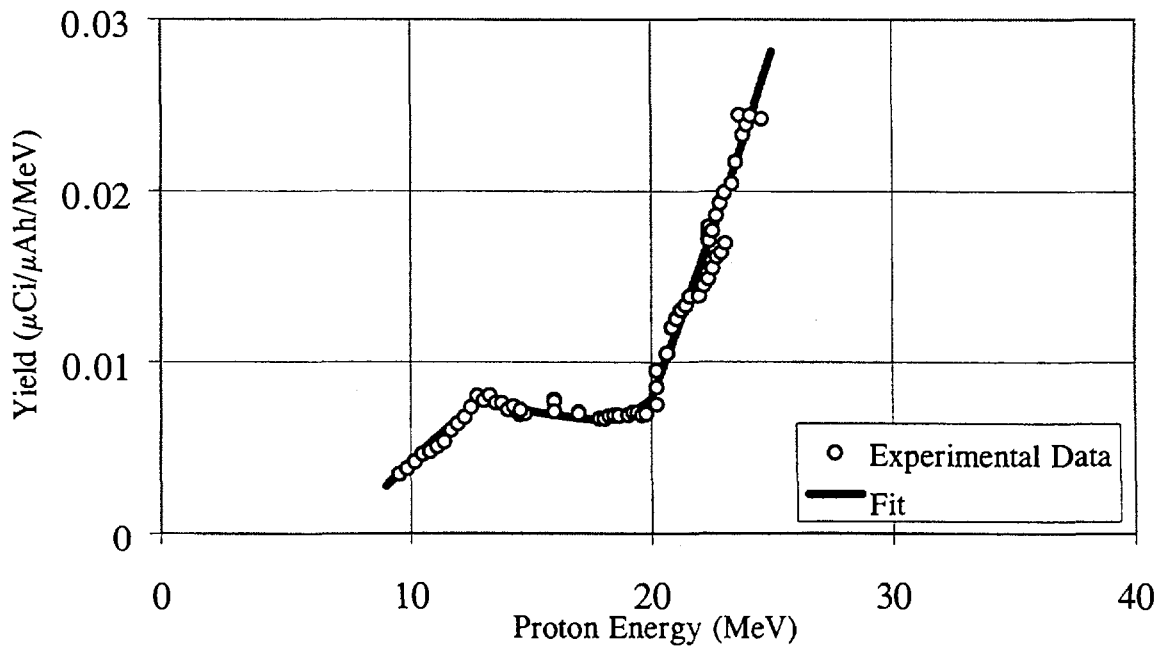


FIG. 6. Extrapolated ^{96}Tc yields to enriched ^{100}Mo (CIS; 97.46%) targets.

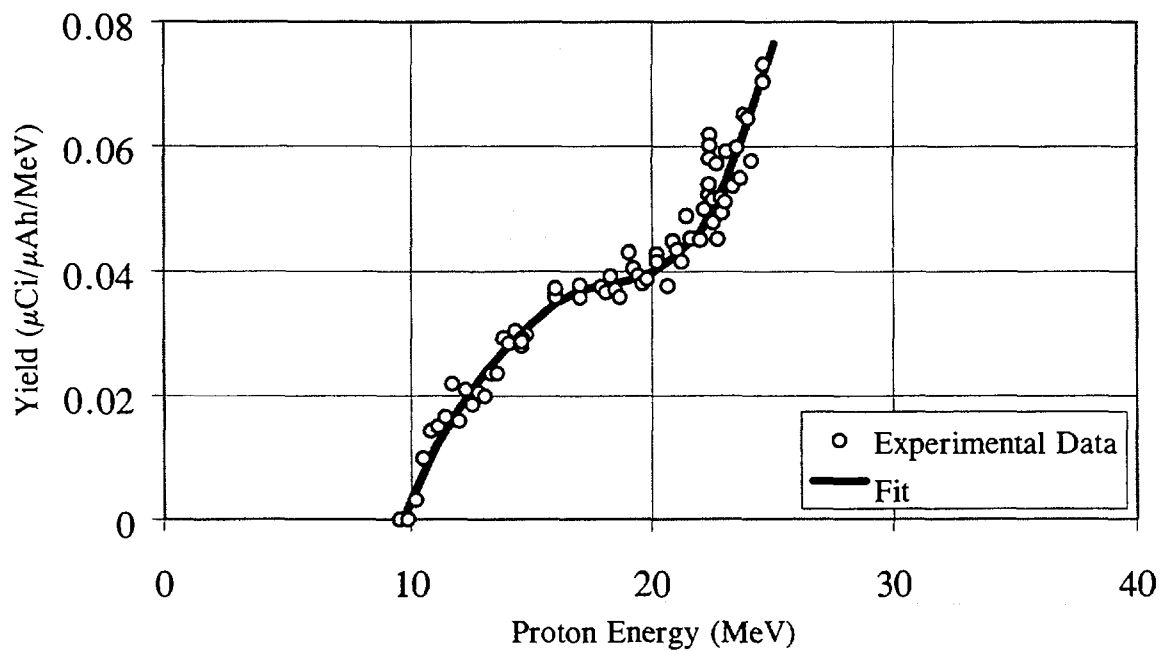


FIG. 7. Extrapolated ^{95}Tc yields to enriched ^{100}Mo (CIS; 97.46%) targets.

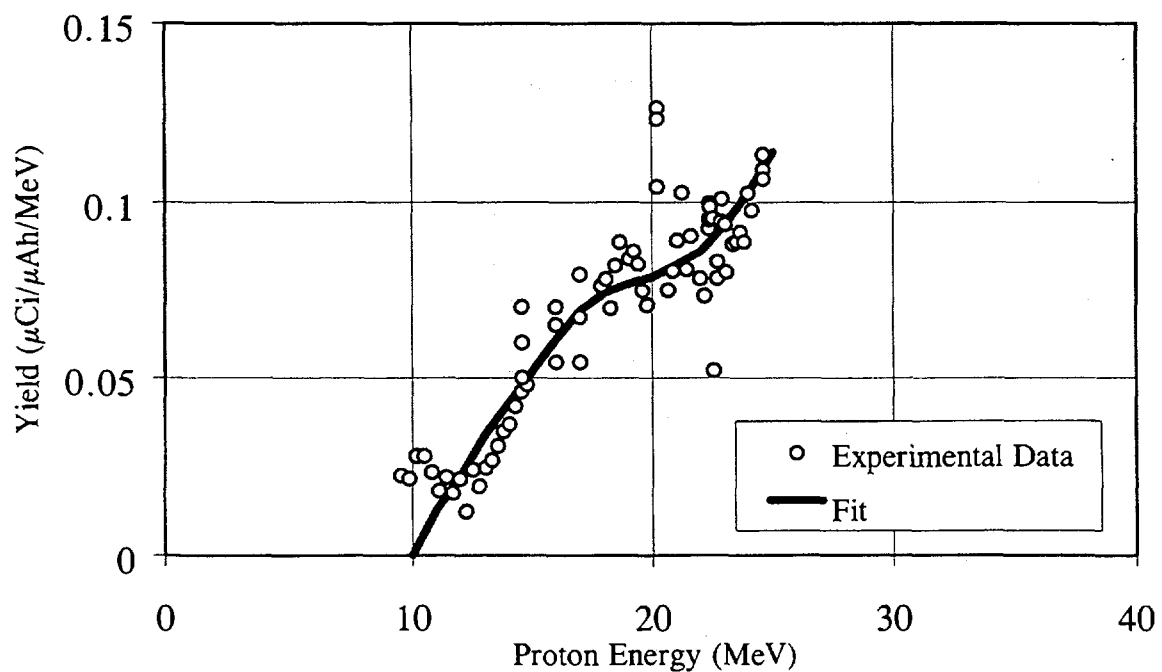


FIG. 8. Extrapolated ^{94}Tc yields to enriched ^{100}Mo (CIS; 97.46%) targets.

TABLE VI. COMPARISON OF MEASURED AND CALCULATED ^{99m}Tc AND ^{96}Tc YIELDS PRODUCED WITH 20.5 MeV PROTONS ON ENRICHED ^{100}Mo TARGETS (CIS; 97.46 %).

Proton Energy ¹ (MeV)	Target Thickness (g/cm ²)	Energy Loss in Target (MeV)	^{99m}Tc Yields (EOB)		^{96}Tc Yields (EOB)	
			Measured (mCi/μAh)	Calculated (mCi/μAh)	Measured (μCi/μAh)	Calculated (μCi/μAh)
19.24	0.155	2.17	4.53 ± 0.72		5.20 ± 0.68	0.0158 ± 0.0095
19.26	0.152	2.12	4.58 ± 0.73		5.01 ± 0.65	0.0254 ± 0.0152
19.36	0.139	1.93	4.26 ± 0.68		4.49 ± 0.58	0.0245 ± 0.0147
19.31	0.145	2.02	4.09 ± 0.65		4.74 ± 0.62	0.0220 ± 0.0132

¹Mean value (see text).

TABLE VII. COMPARISON OF MEASURED AND CALCULATED ^{99m}Tc AND ^{96}Tc YIELDS PRODUCED WITH A 22.2-13.2 THICK TARGET USING ENRICHED ^{100}Mo (CIS; 97.46 %)².

Proton Energy (MeV)	Target Thickness (g/cm ²)	Energy Loss in Target (MeV)	^{99m}Tc Yields (EOB)		^{96}Tc Yields (EOB)	
			Measured (mCi/μAh)	Calculated (mCi/μAh)	Measured (μCi/μAh)	Calculated (μCi/μAh)
22.2 -13.2	0.609	9.0	18.5 ± 7.4		20.6 ± 2.7	0.066 ± 0.040
Radionuclide Purity (%)		>99.999	>99.999		0.00036	0.00035

² Results from radioassays before and after radiochemistry.

TABLE VIII. THICK-TARGET YIELDS AND PURITIES FOR ^{99m}Tc PRODUCED VIA THE $^{100}\text{Mo}(p,2n)$ REACTION USING CIS ENRICHED ^{100}Mo (97.46%) AND 10-MeV TARGET THICKNESSES.³

Target Thickness (Incident/Exit Energy) (MeV)	^{99m}Tc (mCi/μAh)	^{96}Tc (μCi/μAh)	^{95}Tc (μCi/μAh)	^{94}Tc (μCi/μAh)
20 - 10	21.1	0.0676	0.283	0.485
21 - 11	22.5	0.0725	0.317	0.559
22 - 12	23.0	0.0800	0.346	0.625
23 - 13	22.9	0.0904	0.376	0.686
24 - 14	22.1	0.1050	0.409	0.746
25 - 15	20.8	0.1230	0.450	0.808

³Calculations done by integration of yields as given in Table 5.

incident and exit proton energies, calculated using the computer code RANGE [17]. In addition, when limiting the incident proton energy on the ^{100}Mo target to less than 20.5 MeV, ^{96}Tc was the only Tc impurity detected in the target. Seven days after EOB, the cumulative ^{96}Tc yields were measured, converted to EOB, and the measured results also agreed with the calculated values obtained by extrapolation (Table VI). The final radionuclide purity for ^{99m}Tc was determined as > 99.99% at EOB, and can be improved further as a thicker target may be utilized to enhance the production of ^{99m}Tc , rather than ^{96}Tc . Limiting the proton incident energy to <20.5 MeV results, however, in a large penalty in ^{99m}Tc yields.

Further experimental testing with a 22.2-13.2-MeV thick ^{100}Mo targets (CIS; 97.46%), and a comparison of measured and calculated yields were also conducted. The results are summarized in Table VII. Once again, yield and purity measurements demonstrated the capabilities of this accelerator-based method to produce high-quality $^{99\text{m}}\text{Tc}$ for medical use.

In addition, the results of these tests further demonstrated the internal consistency of the excitation data reported here and the ability to predict yield and purity under a variety of target and proton energy conditions. These test results were then utilized in establishing the optimal proton energy and target thickness parameters for the production of $^{99\text{m}}\text{Tc}$.

3.5. Optimization of the production of $^{99\text{m}}\text{Tc}$ from CIS ^{100}Mo (97.46%) targets

In order to maximize $^{99\text{m}}\text{Tc}$ yields and radionuclide purity with <23 MeV protons on CIS-type enriched ^{100}Mo (Table I), a series of calculations for 10-MeV thick targets were performed and the results are given in Table VIII. An inspection of these results indicated an optimal proton energy region of 22-12 MeV, under which the maximum cumulative $^{99\text{m}}\text{Tc}$ yield of 23.0 ± 3.0 mCi/ μAh at EOB, is reached. On the basis of the results given in Table VII and the calculations summarized in Table VIII, we concluded that the optimization of $^{99\text{m}}\text{Tc}$ yield and purity should be performed around the 22-MeV proton energy region, with a 10-MeV thick target. Providing a maximum $^{99\text{m}}\text{Tc}$ yield and purity should be performed around the 22-MeV proton energy region, with a 10-MeV thick target. Providing a maximum $^{99\text{m}}\text{Tc}$ yield and minimizing the level of ^{96}Tc production were the major factors considered in this conclusion.

3.5.1. Production test for $^{99\text{m}}\text{Tc}$ under optimal conditions

Experimental validations of the optimal production conditions defined above, were conducted with 22.4-MeV protons bombarding 22-12 MeV CIS-enriched ^{100}Mo targets. The results are summarized in Table IX, where the calculated $^{99\text{m}}\text{Tc}$ production rate and the level of Tc impurities are given as a function of time. The purity of the $^{99\text{m}}\text{Tc}$ thus produced is very high, >99.99% at EOB, and larger than 99.9% even 24 hours after EOB. This test confirmed the high purity level for $^{99\text{m}}\text{Tc}$ predicted from the excitation function data, and proved once more that the accelerator-based method reported here is suitable for producing $^{99\text{m}}\text{Tc}$ for

TABLE IX. TIME DEPENDENT YIELD AND PURITY FOR $^{99\text{m}}\text{Tc}$ PRODUCED FROM CIS ENRICHED ^{100}Mo (97.46%) VIA THE $^{100}\text{Mo}(p,2n)$ REACTION IN THE 22-12 MeV PROTON ENERGY REGION

Nuclide	EOB	EOB + 6h	EOB + 12h	EOB + 18h	EOB + 24 h
$^{99\text{m}}\text{Tc}$ Yield (mCi/ μAh)	23.0	11.5	5.78	2.89	1.45
$^{99\text{m}}\text{Tc}$ Purity (%)	99.995	99.995	99.993	99.989	99.983
^{96}Tc	0.000348	0.000667	0.00128	0.00245	0.00470
^{95}Tc	0.00150	0.00244	0.00395	0.00640	0.0104
^{94}Tc	0.00272	0.00231	0.00197	0.00167	0.00143
Total Impurity (%)	0.00457	0.00542	0.00720	0.01050	0.01650

medical use. Technetium-96 (4.35 d) was the only impurity detected 48-96 h past EOB by using high-resolution γ -ray spectrometry. No further measurements were made due to the low count rates.

3.5.2. High-resolution gamma-ray spectrometry tests

In some test runs, the ^{100}Mo target was dissolved, and a radiochemical separation of Tc isotopes from the target material, and from other radionuclides formed, was conducted (see section 3.7, below). These procedures were followed by radioassays conducted with high-resolution (Ge) gamma-ray spectrometry methods. The results of these tests are shown in several γ -ray spectra of the directly-made $^{99\text{m}}\text{Tc}$ (Fig. 9, 100-450 keV γ -ray spectrum) and in Fig.10 (enhanced 650-900 keV γ -spectrum for Tc impurities). In addition, a comparison of radioassays was also made with similar γ -ray spectra taken from samples of $^{99\text{m}}\text{Tc}$ eluted from a commercial fission-made $^{99}\text{Mo} \rightarrow ^{99\text{m}}\text{Tc}$ generator, which are shown in Figures 11 and 12, respectively. An analysis of these spectra revealed no detectable differences, suggesting that both accelerator-made and reactor-produced $^{99\text{m}}\text{Tc}$ products would provide similar quality and imaging resolution.

Additional information regarding the variation of $^{99\text{m}}\text{Tc}$ radionuclide purity that would potentially alter the quality of imaging during a 24-h long “usable shelf life” period-assumed for a directly-made source of $^{99\text{m}}\text{Tc}$, is given in Table IX. In this Table, the level of radionuclide purity during different time intervals of the suggested effective shelf life of 24 hours, is given. Although $^{99\text{m}}\text{Tc}$ purity is reduced with time, even at the expiration time of $^{99\text{m}}\text{Tc}$ (24 h past EOB), its radionuclide purity remains above 99.9%, with <0.1% of Tc impurities (mostly ^{96}Tc) present.

Therefore, based upon the data and results presented here, different operational parameters for an accelerator-based method are available to achieve the desired yield and purity levels suggested from this data. The methodology used in this work, by comparing it with a commercial quality reactor-produced $^{99\text{m}}\text{Tc}$, proved the validity of this conclusion.

3.6. Extrapolated $^{99\text{m}}\text{Tc}$ production capabilities

The potential of this new accelerator-based method for the production of $^{99\text{m}}\text{Tc}$, can also be evaluated by using the current and forthcoming capabilities of modern proton accelerators operating with high intensity, mA-beams on targets capable of withstanding several-kW beam power deposition levels. In the 22-12 MeV proton energy region, the

TABLE X. EXTRAPOLATED $^{99\text{m}}\text{Tc}$ YIELDS FOR HIGH-INTENSITY, HIGH-POWER PRODUCTION WITH CIS ENRICHED ^{100}Mo (97.46%) TARGETS IN THE 22-12 PROTON ENERGY REGION¹.

Beam Current (mA)	Target Power (kW)	$^{99\text{m}}\text{Tc}$ Yields per Irradiation Times					
		(Ci/6h) (EOB)	(Ci/6h) (EOB+24h)	(Ci/12h) (EOB)	(Ci/12h) (EOB+24h)	(Ci/18h) (EOB)	(Ci/18h) (EOB+24h)
1	10	99.6	6.28	150	9.46	175	11.0
2	20	199	12.6	299	18.9	349	22.0
5	50	498	31.4	748	47.2	874	55.1
10	100	996	62.8	1,496	94.4	1,747	110.2

¹ Corrected for decay during bombardment.

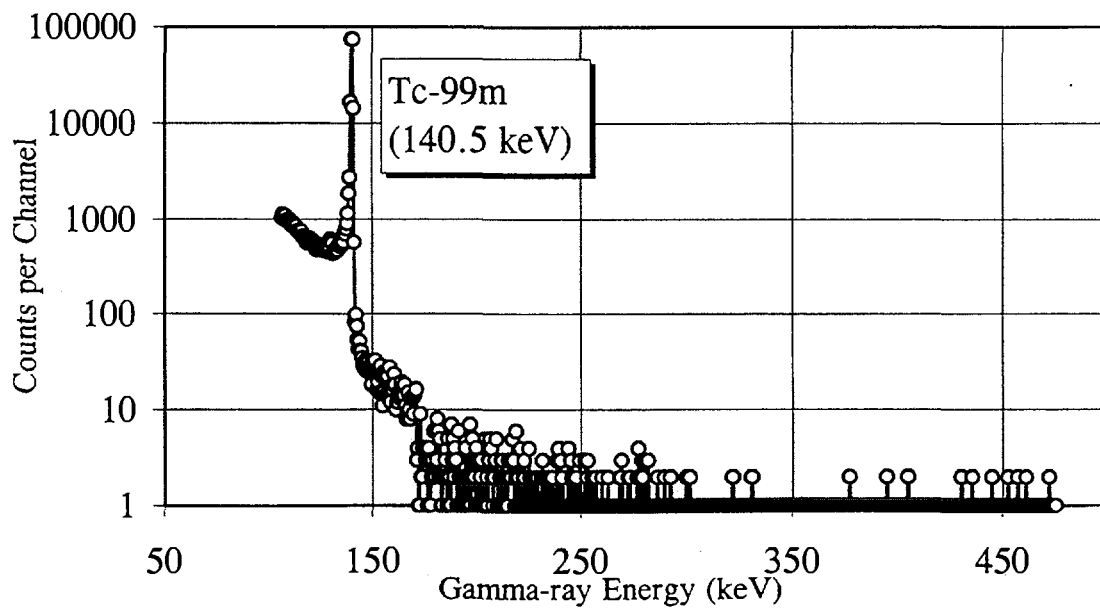


FIG. 9. Gamma-ray spectrum of accelerator-produced ^{99m}Tc from an enriched ^{100}Mo (CIS; 97.46%) thick (22.2-13.2 MeV) target Radioassay at 25 h after EOB.

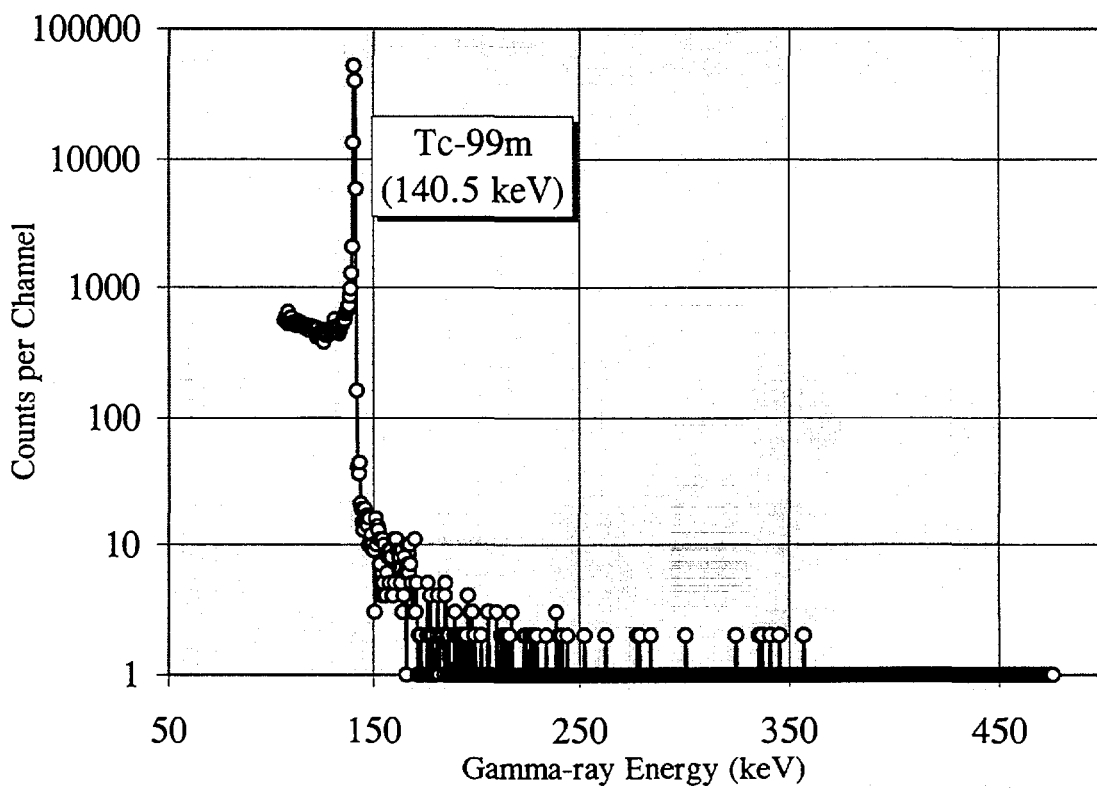


FIG. 10. Gamma-ray spectrum of generator-produced ^{99m}Tc . Radioassay at 24 h after elution.

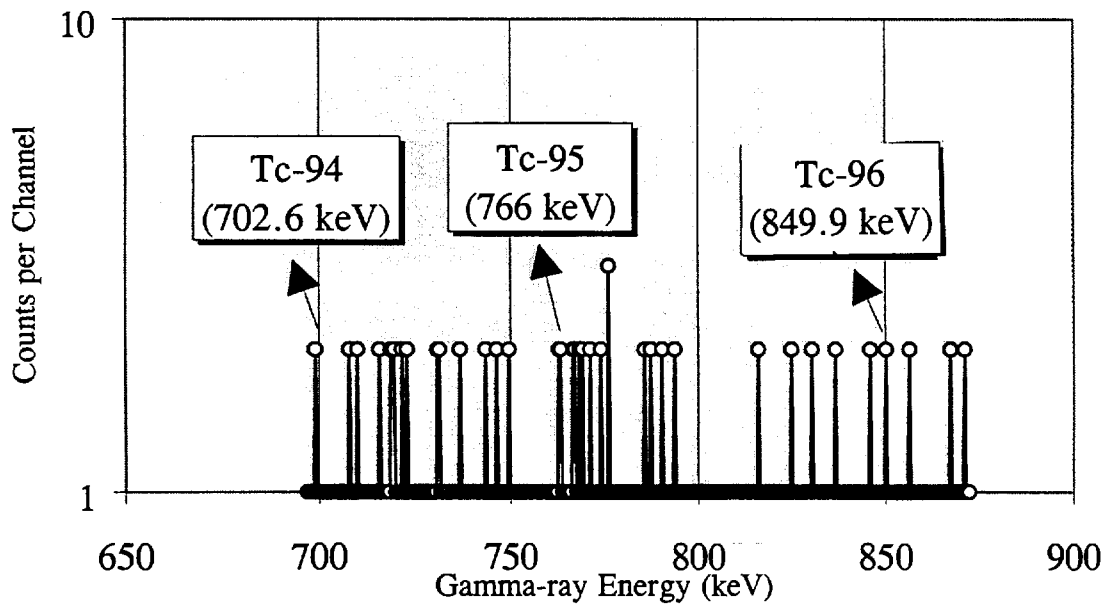


FIG. 11. Gamma-ray spectrum of accelerator-produced Tc impurities from an enriched ^{100}Mo (CIS; 97.46%) thick (22.2-13.2 MeV) target. Radioassay at 25 h after EOB.

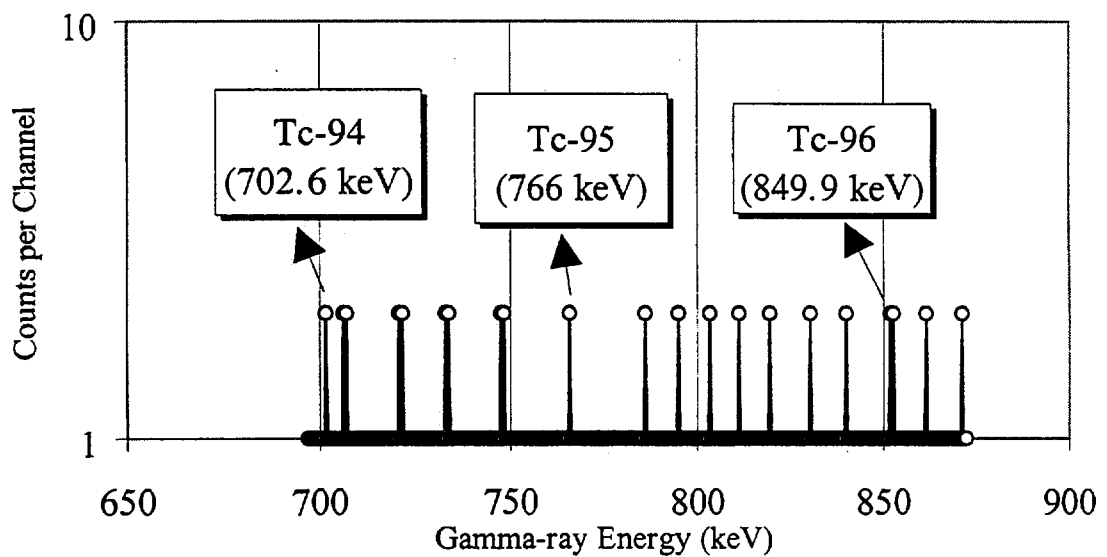


FIG. 12. Gamma-ray spectrum of generator-produced Tc impurities. Radioassay at 24 h after elution.

cumulative ^{99m}Tc yields per target were extrapolated to higher beam intensities and target power using enriched ^{100}Mo (97.46%). Results of these extrapolations, using current accelerator and target capabilities, and those under development, are summarized in Table X.

The use of a large 2-mA cyclotron beam current for radioisotope production was recently reported [19, 20], and higher currents up to 7 mA are being tested and developed [20]. Using high beam current and high power target technologies available today, as many as several hundreds Ci of ^{99m}Tc could be produced each day, indicating that the potential for local and/or regional supply with directly-produced ^{99m}Tc is technically feasible.

3.7. Target radiochemistry: separation and purification of directly-made ^{99m}Tc

The development and testing of rapid and efficient chemical separation methods for Mo-Tc radioactivity's is not a major challenge for the establishment of an accelerator-based method to produce ^{99m}Tc . Since the development of the $^{99}\text{Mo} \rightarrow ^{99m}\text{Tc}$ generator system in the late 1960's by Richards et al, [3], there is ample and well documented information on methods apt for implementation and that can be easily subjected to automation to provide safe, rapid, and efficient Mo-Tc radiochemistry. Therefore, the radiochemistry used in this study was based upon this wealth of information, and was completed in less than 1 hour. This method was not automated, provided an efficient separation of Tc from Mo, an easy recovery of the enriched ^{100}Mo material from an aqueous solution, and was proven to be reliable. The steps and the timing of the method are summarized in Table XI. However, no efforts were made to complete the recovery cycle of the dissolved ^{100}Mo target material and, therefore, this task needs to be investigated. It is suggested, however, that there is ample experience in recovering and reusing enriched materials during commercial cyclotron production activities, and that the properties of Mo as a target, makes this task achievable.

As of this date, the specific activity of directly-made ^{99m}Tc , using the optimal conditions and the radiochemistry generally described above, has not been measured. A high specific activity is desirable as many of the synthesis for various ^{99m}Tc labeled radiopharmaceuticals may be affected. Studies using on-line nuclear spectroscopy methods to measure the relative ratio of excited states of ^{99}Tc (2.4×10^5 a) and ^{99m}Tc produced by proton bombardment of CIS enriched ^{100}Mo , are in progress and will be reported elsewhere [21]. Preliminary results and the nuclear properties indicated that a predominant formation of the ^{99m}Tc state is likely, which would suggest that an adequate specific activity can be achieved. Furthermore, the production of ^{99m}Tc from ^{100}Mo targets is conducted in a no-carrier-added condition.

TABLE XI. RADIOCHEMISTRY FOR SEPARATION OF ^{99m}Tc FROM Mo TARGETS

Radiochemistry Step	Time (min)	Elapsed Time (min)
^{100}Mo Target Dissolution with H_2O_2 (30%)	< 5	< 5
^{99m}Tc Separation by Solvent Extraction (MEK)	< 15	< 20
^{99m}Tc Purification by Ion Exchange	< 15	< 35
^{99m}Tc Chemical Formulation in Isotonic Saline	< 10	< 45
^{100}Mo Recovery in Aqueous Solution	< 10	n/a

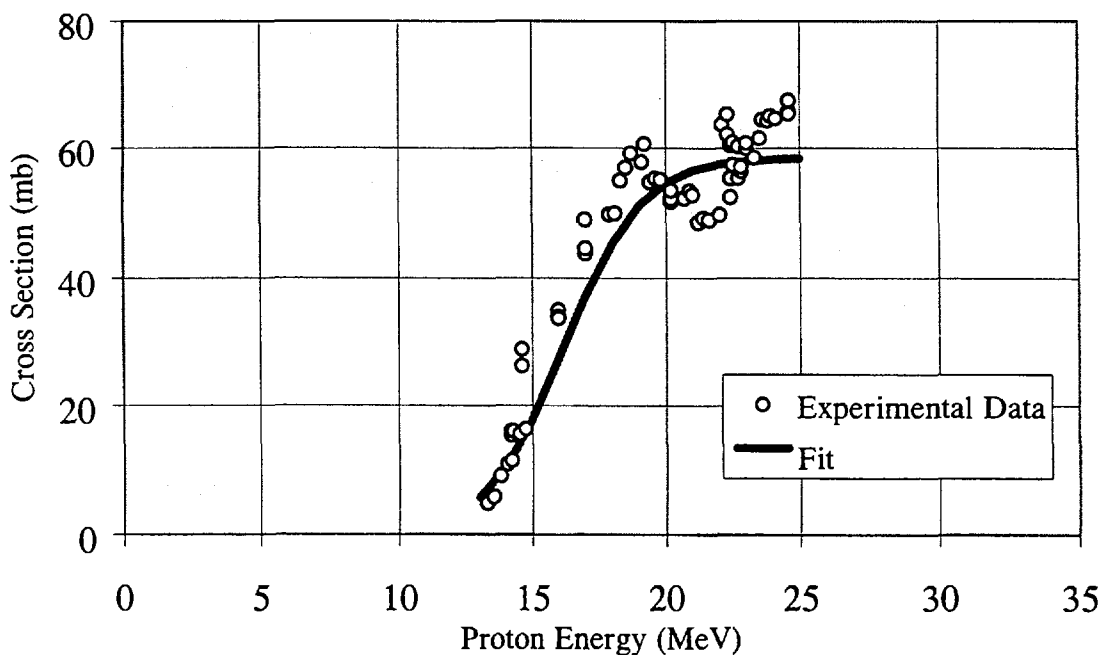


FIG. 13. Excitation function for the $^{100}\text{Mo}(p,pn)^{99}\text{Mo}$ reaction ($Q = -8.3$ MeV).

3.8. Molybdenum-99 production

In addition to completing the experimental work regarding the production of Tc isotopes from Mo targets, the production of ^{99}Mo via the $^{100}\text{Mo}(p,pn)^{99}\text{Mo}$ ($Q = -8.3$ MeV) as a potential alternative method, was also investigated. The results of the cross section measurements were listed in Table IV and are shown in Fig. 13. The cumulative yield of ^{99}Mo from CIS enriched ^{100}Mo (97.46%) targets in the 25 to 13 MeV proton energy region, was calculated as $360 \mu\text{Ci}/\mu\text{Ah}$. This result compared well with previously determined yields using natural Mo targets [6]. However, this accelerator-based yield is too low to be competitive with reactor production of ^{99}Mo , which is estimated as 32 Ci/h using neutron-induced fission methods [22]. In addition, ^{99}Mo would be produced in the same matrix as the enriched (and expensive) ^{100}Mo target material, forcing recovery for recycling. Furthermore, the resulting specific activity would be low and not practical for the current generation of high-specific activity fission-produced $^{99}\text{Mo} \rightarrow ^{99m}\text{Tc}$ generators. Finally, if natural Mo is used to avoid some of the above indicated conditions, the yield would be lowered by a factor of ≈ 10 . An alternative to this approach using proton-induced fission methods, is under study [11,12].

3.9. Future work

Additional large-scale production experiments using enriched ^{100}Mo targets and incident proton energies in the 20-23 MeV region should be undertaken to provide further assurances on an optimal condition for the production of ^{99m}Tc . In these runs, further radioassays to confirm radionuclide purity, specific activity, labeling yields, and imaging characteristics shall be included. Radiochemistry methods must be further evaluated and optimized to confirm that automated, rapid, and efficient processing and recovery of expensive target material are available. Furthermore, the economic and logistical aspects on the potential use of directly-made ^{99m}Tc should be ascertained. Finally, the potential impact of this technique in developing regions must be evaluated. Most if not all these regions are

depending on foreign supply based on the operation of few commercial reactors, and many at present rely on aging reactor facilities facing decommissioning. Accelerator facilities capable of undertaking this operation are more likely to succeed than new or reconditioned reactors in obtaining support and funding, because modern accelerators are capable of supporting a broader spectrum of diagnostic and therapeutic nuclear medicine applications than reactors. Besides, given the current efforts in developing nations to improve medical technologies, accelerator sources are more likely to succeed in securing core support, as they can be applied to many other science & technology development programs.

4. CONCLUSIONS

The production of directly-made ^{99m}Tc via $^{100}\text{Mo}(p,2n)$ reaction on enriched ^{100}Mo targets in a cyclotron with <25 MeV protons has been demonstrated. The detailed excitation function study indicates that with 97.46 % enriched ^{100}Mo , high production rate (a cumulative ^{99m}Tc yield of 23.0 ± 3.0 mCi/ μAh at EOB) and high purity (>99.99% at EOB, and >99.9% within 24 h after EOB) are reachable in the yield-optimized proton energy region of 22 to 12 MeV. The directly-made ^{99m}Tc was proved to be of excellent radionuclidic purity as compared with reactor-made commercial $^{99}\text{Mo} \rightarrow ^{99m}\text{Tc}$ generator materials.

Instant ^{99m}Tc produced in this fashion would have to be produced in regional/centralized accelerator facilities limiting the supply to local/regional users. In comparison to existing reactor and generator techniques, this method would have several economical advantages as it would minimize nuclear waste production and management costs as well as public and environmental health concerns associated with nuclear reactors.

REFERENCES

- [1] BEAVER, J.E., HUPF, H.B., Production of Tc-99m on a medical cyclotron: a feasibility study, *J. Nucl. Med.* **12(11)** (1971) 739-741.
- [2] ALMEIDA, G.L., HELUS, F., On the production of Mo-99 and Tc-99m by cyclotron, *Radiochem. Radioanal. Lett.* **28(3)** (1977) 205-214.
- [3] RICHARDS, P. In: "The Technetium-99m Generator". Andrews, G.A., Kniseley, J.W., and Wagner H.N. Jr., (Eds.). U.S. Atomic Energy Commission (1966).
- [4] LAGUNAS-SOLAR, M.C., et al., "Accelerator production of molybdenum-99 as a non-reactor source of Mo-99 \rightarrow Tc-99m generators". (Abstract). IX Congress of the Latin American Association of Biology and Nuclear Medicine. October 8-11, 1989, Santiago, Chile.
- [5] LAGUNAS-SOLAR, M.C., "Cyclotron production of Tc-99m and Mo-99 for nuclear medicine applications: a new alternative to reactor-based methods". (Abstract). 15th. Annual Western Regional Meeting of the Society of Nuclear Medicine, Nov. 1-4, 1990, Long Beach, CA. See: *J. Clinical Nuclear Medicine* **15(10)** (1990) 769.
- [6] LAGUNAS-SOLAR, M.C., et al., Cyclotron production of NCA ^{99m}Tc and ^{99}Mo . An alternative non-reactor supply source of instant ^{99m}Tc and $^{99}\text{Mo} \rightarrow ^{99m}\text{Tc}$ generators, *J. Appl. Radiat. Isot.* **42(7)** (1991) 643-657.
- [7] LAGUNAS-SOLAR, M.C., et al., "Accelerator production of Technetium-99m. targetry and radiochemistry effects on yield and purity (Abstract)". 13th International Conference on the Application of Accelerators in Research & Industry (November 7-10, 1994). Denton, Texas, USA.
- [8] LAGUNAS-SOLAR, M.C., Production of Tc-99m and Mo-99 for nuclear medicine applications via accelerators as an option to reactor methods, *J. Radiation Protection in Australia*, **13(1)** (1995) 16-25.

- [9] LAGUNAS-SOLAR, M.C. et al., "An update on the direct production of Tc-99m with proton beams and enriched Mo-100 targets". Annual Meeting of the American Nuclear Society (June 16-20, 1996), Reno, Nevada, USA.
- [10] EGAN G., JAMIESON, C., LAGUNAS-SOLAR, M.C., An investigation into the technical feasibility of cyclotron production of Technetium-99m, Journal of Australia & New Zealand Society of Nuclear Medicine (March 1994) 25-31.
- [11] LAGUNAS-SOLAR, M.C. et al., "Proton fission for the accelerator production of Mo-99". (Abstract). 205th ACS National Meeting, March 28-April 2, 1993, Denver, Colorado. Book of Abstract # 66.
- [12] LAGUNAS-SOLAR, M.C. et al., "Cyclotron production of molybdenum-99 via proton-induced uranium-238 fission". 1996 Annual Meeting of the American Nuclear Society, June 6-12, 1996, Reno, Nevada.
- [13] WILLIAMSON, C., et al., Saclay Report No.CEA-R-3042, (1966).
- [14] GREENE, M.W., LEBOWITZ, E., Protons reactions with copper for auxiliary cyclotron beam monitoring, Int. J. Appl. Rad. Isot. **23** (1972) 342-344.
- [15] JUNGEMAN, J.A. et al., Time-of-flight facility for the absolute measurement of the beam energy of a medium-energy cyclotron, Nucl. Instr. and Meth. **204** (1982) 41.
- [16] ROMERO, J.L. et al., A simple time-of-flight method to measure the beam energy of a cyclotron, Nucl. Instr. and Meth. **100** (1972) 551.
- [17] CROCKER NUCLEAR LABORATORY COMPUTER CODE (RANGE) (J. Lewis, August 1985).
- [18] LEVKOVSKII, V.N., "Activation cross section of nuclides with average masses (A=40-100) by protons and alpha particles with average energies (E=10-50 MeV), Inter Vesi, Moscow, Russia, (1991), p.155.
- [19] JONGEN, Y. et al., High intensity H⁻ cyclotrons for radioisotope production, Ionizing Radiation **15(3)** (1989) 65-74.
- [20] JONGEN, Y. et al. Consultants Meeting of IAEA, (April 10-12, 1997), Faure, South Africa.
- [21] LAGUNAS-SOLAR, M.C., ZENG, N.X., CASTANEDA, C.M., "Determination of specific activity of accelerator-made ^{99m}Tc by on-line nuclear spectroscopy methods". (Manuscript in Preparation).
- [22] MUNZE, R. et al., Large scale production of fission Mo-99 by using fuel elements of a research reactor as starting material, Int. J. Appl. Rad. Isot. **35** (1984) 749-754.